

# Intrinsic Data Constraints and Upper Bounds in Binary Classification Performance

Fei Jing,<sup>1,2</sup> Zi-Ke Zhang,<sup>3,4,\*</sup> and Qingpeng Zhang<sup>1,2,†</sup>

<sup>1</sup>*Musketeers Foundation Institute of Data Science,  
The University of Hong Kong, Hong Kong SAR, China*

<sup>2</sup>*Department of Pharmacology and Pharmacy,  
The University of Hong Kong, Hong Kong SAR, China*

<sup>3</sup>*College of Media and International Culture,  
Zhejiang University, Hangzhou 310058, China*

<sup>4</sup>*Research Center for Digital Communications,  
Zhejiang University, Hangzhou 310058, China*

## Abstract

The structure of data organization is widely recognized as having a substantial influence on the efficacy of machine learning algorithms, particularly in binary classification tasks. Our research provides a theoretical framework suggesting that the maximum potential of binary classifiers on a given dataset is primarily constrained by the inherent qualities of the data. Through both theoretical reasoning and empirical examination, we employed standard objective functions, evaluative metrics, and binary classifiers to arrive at two principal conclusions. Firstly, we show that the theoretical upper bound of binary classification performance on actual datasets can be theoretically attained. This upper boundary represents a calculable equilibrium between the learning loss and the metric of evaluation. Secondly, we have computed the precise upper bounds for three commonly used evaluation metrics, uncovering a fundamental uniformity with our overarching thesis: the upper bound is intricately linked to the dataset's characteristics, independent of the classifier in use. Additionally, our subsequent analysis uncovers a detailed relationship between the upper limit of performance and the level of class overlap within the binary classification data. This relationship is instrumental for pinpointing the most effective feature subsets for use in feature engineering.

---

\*Electronic address: zkz@zju.edu.cn

†Electronic address: qpzhang@hku.hk

Machine learning research has predominantly concentrated on enhancing model accuracy, yet the predictability of machine learning problems remains insufficiently understood [1–4]. A thorough quantification of predictability is paramount for the thoughtful design, training, and deployment of machine learning models, shedding light on the capabilities and limitations of AI in practical scenarios.

Conventional machine learning has often favored error-based metrics as objective functions. However, these metrics have proven to have a negligible impact on optimization outcomes [5] and are prone to complications arising from imbalanced datasets in classification challenges [6]. This recognition has sparked a surge in research directed at AUC maximization within classification tasks [7], spawning a variety of learning frameworks [8], methodologies [9], optimization techniques [10], and their successful implementation in a myriad of fields [11]. Theoretical insights have also been advanced regarding consistency [12] and bounding generalization errors [13].

Although research has made strides in optimizing binary classifiers and demonstrating that an optimal classifier produces a convex ROC curve [14], the maximal AUC remains undisclosed. While efforts to probe link predictability using methods such as information entropy [15] and random turbulence [16] are notable, their reliance on stringent assumptions limits their applicability to extensive, real-world datasets. A gap persists in analytically defining the general predictability of machine learning in practical applications.

This paper seeks to fill this void by theoretically establishing the upper bounds for the receiver operating characteristic (ROC) curve, the precision-recall (PR) curve, and accuracy—a commonly used performance metric. Binary classification, a fundamental machine learning task that segregates entities into two distinct categories, serves as our focus due to its broad applicability. Our goal is to discern a quantifiable link between data’s intrinsic patterns and the ultimate efficacy of binary classifiers—a connection that has remained obscure [14, 17, 18]. We approach the problem by equating the determination of binary classification’s upper bound to solving a classic 0-1 knapsack problem via a greedy algorithm. The derived ROC curve thereby adheres to the optimal ROC convex hull concept as discussed in [19]. Similar methodologies are applied to ascertain the optimal PR curve and accuracy through enumeration.

Our investigation extends to the robustness of our proposed methods under the complementarity principle [20], a concept drawing from the Pauli exclusion principle. We illustrate analytically that the divergence between training and testing datasets significantly impacts binary classifiers’ performance. Experiments with four real-world datasets corroborate the practicality and extendibility

of our methods in deducing the performance upper bounds of binary classifiers.

Our analysis further identifies a direct correlation between the overlap of positive and negative instances and the performance ceiling of a dataset. Specifically, reduced overlap translates to augmented predictive capacity and likely enhanced model performance. Conversely, when positive and negative instances are indistinguishable, model efficacy is tantamount to random chance. In feature engineering, we observe that incorporating novel features (feature selection) can mitigate this overlap, thereby elevating the dataset’s performance potential. In contrast, manipulations using existing features, like feature extraction, do not affect the overlap or the upper limits of evaluation metrics.

## Results

### Preliminaries.

Consider a binary dataset  $\mathcal{S} = \{(x_i, y_i) \mid i = 1, 2, \dots, m\}$ , where each instance consists of a  $k$ -dimensional feature vector  $x_i = (x_{i,1}, x_{i,2}, \dots, x_{i,k}) \in \mathcal{X}$  and a corresponding class label  $y_i \in \{1, -1\}$ . We denote  $\mathcal{X}$  as the domain comprising all unique feature vectors in  $\mathcal{S}$ . For a given feature vector  $x_i$ ,  $\mathcal{P}(x_i)$  and  $\mathcal{N}(x_i)$  indicate the count of positive and negative samples, respectively. Additionally, the entire dataset contains  $n_+$  positive and  $n_-$  negative samples. The proportion of positive instances for a particular feature vector  $x_i$  is expressed as  $p_+(x_i) = \mathcal{P}(x_i)/(\mathcal{P}(x_i) + \mathcal{N}(x_i))$ .

Binary classification models function by assigning a feature vector  $x_i$  to a binary class. These models are broadly categorized into two types: continuous and discrete classifiers. Continuous classifiers employ a real-valued function  $f : \mathcal{X} \rightarrow \mathbb{R}$  to gauge the likelihood of an instance belonging to each class, based on a predefined threshold  $t$ . Examples of continuous classifiers include logistic regression [21, 22] and neural networks [23, 24]. On the other hand, discrete classifiers directly generate binary outcomes, such as support vector machines (SVM) [3, 25] and decision trees [26, 27].

### Boundary of Evaluation Measures.

To assess the performance of binary classifiers, we investigate three prominent evaluation metrics: the ROC curve, the PR curve, and accuracy. Each of these metrics evaluates classifier performance from distinct perspectives.

**Upper Bound of ROC Curve.** The ROC curve is a fundamental tool for displaying the discriminative capacity of a binary classifier across various threshold settings [14, 18]. It delineates the

trade-off between sensitivity (true positive rate) and specificity (true negative rate), assisting in the selection of an optimal threshold. The area under the ROC curve (AUC-ROC) quantifies the probability that a randomly chosen positive instance is ranked higher than a negative instance, serving as a summary measure of classifier performance across all thresholds [28, 29]. We have established the exact upper bound of the AUC ( $AR^u$ ) for a given binary dataset  $\mathcal{S}$ , expressed as (refer to *SI Appendix, Optimal ROC Curve* for the detailed mathematical derivation):

$$AR^u = \frac{1}{2n_+n_-} \sum_{x_i, x_j} \max \left\{ \mathcal{P}(x_i)\mathcal{N}(x_j), \mathcal{P}(x_j)\mathcal{N}(x_i) \right\}, \quad (1)$$

where  $x_i$  and  $x_j$  are two arbitrary feature vectors from  $\mathcal{S}$ . This upper bound is attainable by a binary classifier if and only if it satisfies  $f_{AR}^*(x_i) \sim p_+(x_i)$ , where  $f(x_i) \sim f'(x_i)$  denotes that  $f(x_i) > f(x_j)$  if and only if  $f'(x_i) > f'(x_j)$  for every pair  $(x_i, x_j)$  in  $\mathcal{S}$ .

Figure 1A-1D depicts the results of in-sample experiments featuring a suite of well-known binary classifiers, including XGBoost, Multilayer Perceptron (MLP), Support Vector Machine (SVM), Logistic Regression, Decision Tree, Random Forest, KNN, and Naive Bayes. These classifiers were tested with a variety of objective functions. In addition, the theoretical upper limits were computed in accordance with Eq. 1. Across all cases, the theoretical upper bounds exceeded the performance of each classifier as measured by the ROC curves, thereby confirming the accuracy of our theoretical predictions.

**Upper Bound of PR Curve.** Unlike the ROC curve, the PR (precision-recall) curve is particularly useful for evaluating performance on imbalanced datasets where one class significantly outnumbers the other [30]. The PR curve illustrates the precision-recall trade-off as the classification threshold is adjusted. We demonstrate that the theoretical upper bound of the area under the PR curve (AUC-PR,  $AP^u$ ) for a binary dataset  $\mathcal{S}$  is given by (see *SI Appendix, Optimal PR Curve* for the mathematical proof):

$$AP^u = \frac{1}{2n_+} \sum_{i=1}^m p_+(x_i^*) \left( \frac{1}{i-1} \sum_{j=1}^{i-1} p_+(x_j^*) + \frac{1}{i} \sum_{j=1}^i p_+(x_j^*) \right), \quad (2)$$

where  $x_i^*$  and  $x_j^*$  are feature vectors sorted according to  $f_{AP}^*(x_i)$ . This upper bound is achievable by a binary classifier if and only if it satisfies  $f_{AP}^*(x_i) \sim p_+(x_i)$  for every  $x_i \in \mathcal{S}$ , mirroring the condition for  $AR^u$ .

Fig. 1E-1H presents the experimental findings with aforementioned representative binary classifiers against the theoretical upper bounds derived using Eq. 2. As with the ROC curve, the experimental results for binary classification do not exceed the theoretical upper bounds ( $AP^u$ ), thereby supporting the validity of our theoretical derivation.

**Upper Bound of Accuracy.** Accuracy (AC) is the fraction of instances correctly classified by the classifier [31, 32]. We have derived its theoretical upper bound (detailed in *SI Appendix, Accuracy*):

$$AC^u = \frac{1}{m} \sum_{x_i} \max \left\{ \mathcal{P}(x_i), \mathcal{N}(x_i) \right\}. \quad (3)$$

This upper limit is attainable if, and only if, the optimal classifier dictates that:

$$f_{AC}^*(x_i) = \begin{cases} 1 & \mathcal{P}(x_i) \geq \mathcal{N}(x_i) \\ -1 & \mathcal{P}(x_i) < \mathcal{N}(x_i) \end{cases},$$

for each  $x_i$  in  $\mathcal{S}$ . Table 1 compares the accuracy achieved by various classifier configurations against the theoretical upper bounds, further substantiating the rigour of our theoretical derivation.

### Unified Optimal Classifier.

The theoretical foundation of optimal classifiers demonstrates their alignment with the common objective functions including Square loss, Logistic loss, Hinge loss, and Softmax loss [1] (refer to *SI Appendix, Objective Functions* for additional details). Specifically, the optimal classifiers for both the ROC and PR curves are congruent, denoted as  $f_{AR}^* \equiv f_{AP}^*$ . This implies that continuous binary classifiers converge to a unified optimal form for each feature vector  $x_i \in \mathcal{S}$ , symbolized as  $g_{\text{Square}}^* \equiv g_{\text{Logistic}}^* \sim p_+(x_i) \equiv f_{AR}^* \equiv f_{AP}^*$ , where  $g^*$  represents the objective function. Similarly, discrete binary classifiers are equivalent, denoted as  $g_{\text{Hinge}}^* \equiv g_{\text{Softmax}}^* \equiv f_{AC}^*$ .

From this, we can deduce a universal representation for any optimal classifier, encompassing both continuous and discrete forms, that achieves the best performance across various objective functions and evaluation metrics:

$$\mathcal{F}^*(x_i) = \begin{cases} 1 & f^*(x_i) \geq 0 \\ -1 & f^*(x_i) < 0 \end{cases}, \quad (4)$$

where  $f^*(x_i) = \frac{\mathcal{P}(x_i) - \mathcal{N}(x_i)}{\mathcal{P}(x_i) + \mathcal{N}(x_i)}$  is the derived optimal classifier that minimizes loss and maximizes performance across various objective functions and evaluation metrics. Furthermore, the classifier  $f^*(x_i)$  can also be seen as determining the optimal threshold for the optimal continuous classifier. A related study published in PNAS [33] also derived this threshold by employing a Fermi-Dirac type data distribution coupled with maximum likelihood assumptions.

Eq. 4 underscores the synergy between the learning process, which is steered by objective functions, and the evaluation process within the realm of binary classification. The efficacy of a binary classifier, irrespective of its computational complexity or efficiency, is inherently bound by the selected objective function and the intrinsic properties of the dataset. This establishes a performance ceiling dictated by both the chosen evaluation metric and the data’s innate characteristics.

### **Sensitivity Analysis in the Out-of-Sample Context.**

Note that, the aforementioned binary boundary theory is derived in an in-sample context, where the classification and validation are based on the full dataset. As a consequence, a fundamental question remains: To what extent can the boundary theory derived from full dataset be applied to the out-of-sample scenario? We further perform out-of-sample validation, and sensitivity analysis with various random separation ratio.

Specifically, we divide the data to a training set ( $\mathcal{S}_{train}$ ) and a test set ( $\mathcal{S}_{test}$ ). The model is trained on the training set and validated on the test set. The performance of the learned classifier varies given different statistical characteristics of the data in the test set, even though it is trained guided by the objective function based on the data organization in the training set. Hence, the generalization ability of the classifier is determined by the gap between data distributions of training and test sets [34, 35]. Here, we perform extensive sensitivity analysis of the optimization and evaluation process. Without loss of generality, we focus on the analysis of Hinge loss and accuracy (AC).

We start by defining  $\mathcal{P}_{train}(x_i)$  and  $\mathcal{N}_{train}(x_i)$  as the number of positive and negative instances with feature vector  $x_i$  in  $\mathcal{S}_{train}$ ,  $\mathcal{P}_{test}(x_i)$  and  $\mathcal{N}_{test}(x_i)$  as the number of positive and negative instances with feature vector  $x_i$  in  $\mathcal{S}_{test}$ . Given a discrete classifier  $f(x_i)$ , we further define  $\Delta_{train}^f$  as the bias between the actual Hinge loss and the optimal loss in  $\mathcal{S}_{train}$ . Similarly,  $\Delta_{test}^f$  is defined as the bias between the actual accuracy and optimal accuracy in  $\mathcal{S}_{test}$ . Therefore, the question is converted to minimizing the summation of the two errors

$$\Delta = \min_f (\Delta_{train}^f + \Delta_{test}^f). \quad (5)$$

Apparently, there must exist a *perfect* classifier that reaches the minimum Hinge loss and highest accuracy for both training set and test set when  $\Delta = 0$ . In addition,  $\Delta = 0$  if and only if (detailed mathematical proof see *SI Appendix, Sensitivity Analysis*)

$$\begin{cases} \mathcal{P}_{train}(x_i) \geq \mathcal{N}_{train}(x_i) \\ \mathcal{P}_{test}(x_i) \geq \mathcal{N}_{test}(x_i) \end{cases} \quad \text{or} \quad \begin{cases} \mathcal{P}_{train}(x_i) \leq \mathcal{N}_{train}(x_i) \\ \mathcal{P}_{test}(x_i) \leq \mathcal{N}_{test}(x_i) \end{cases} \quad (6)$$

for every  $x_i \in \mathcal{S}$ . Eq. 6 shows that the upper bound of binary classification on a specific data, i.e.  $\Delta = 0$ , can be reached only if the distribution of data between the training and test sets are consistent. Hence, when the training set and the test set share a similar data structure, the trained classifier can exhibit a phenomenon known as *benign overfitting* [36], showcasing exceptional generalization capability. However, the trained classifier in real scenarios often can approach the upper limit of corresponding loss function ( $\Delta_{train}^f=0$ ), but difficult to simultaneously achieve the upper bound of performance on the test set ( $\Delta_{test}^f=0$ ) because of the discrepancies between the distributions of data in training and test sets.

In Fig. 2, we investigate at length the characteristics of both training and test sets in order to comprehensively understand the generalization ability of the proposed boundary theory. It shows that, the theoretical optimal loss for  $\Delta$  is smaller than that of any representative classier, suggesting that the predictability of available classifiers are still a certain distance from the theoretical upper limit, both for a specific division (i.e.  $|\mathcal{S}_{train}|/|\mathcal{S}| = 70\%$ , Fig. 2A) or all possible random divisions (Fig. 2C). Therefore,  $\Delta_{train}^f$  and  $\Delta_{test}^f$  are respectively equivalent to the learning and generalization differences in supervised machine learning. If one aims at obtaining the upper bound of a given dataset (corresponds to  $\Delta$ ), he or she needs to minimize simultaneously both  $\Delta_{train}^f$  and  $\Delta_{test}^f$  [37]. However, on one hand, it requires fitting training data as much as possible to obtain minimal  $\Delta_{train}^f$ , often leading to the overfitting problem [36, 38], which further dilutes the generalization ability (corresponds to greater  $\Delta_{test}^f$  and more distant from the upper bound). On the other hand, one may try to solve such dilemma by early-stopping, dropout or adding regularization items [38, 39], resulting in a greater learning loss (corresponds to larger  $\Delta_{train}^f$ ), leaving an unstable prediction.

Fig. 2D shows a general increase of learning loss with the size of training set ( $|\mathcal{S}_{train}|$ ), which converges to a certain limit if the feeding schema is sufficient enough. Comparatively, the upper bound ( $AC^u$ ) monotonically increases with  $|\mathcal{S}_{train}|$  (Fig. 2E), which agrees with the common sense that more knowledge can be extracted by adding more sources. The good agreements are

additional proved theoretically by giving an arbitrary parameter governing the ratio of random divisions (represented by solid lines in Fig. 2D-2F, see also *SI Appendix, Random Division*). Furthermore, Fig. 2F shows that the optimal error ( $\Delta$ ) will be achieved when the training set is either adequate large or small enough as its expectation is symmetric based on *SI Appendix, Eq. 56*.

### Effect of Overlapping Ratio of Samples.

The relationship between the distribution pattern of feature vectors, specifically the overlapping ratio of data samples, and the expected upper bounds ( $\text{AR}^u$ ) is investigated. To ascertain the minimum and maximum values of  $\text{AR}^u$ , we formulate two optimization problems as follows:

$$\text{AR}_{\min}^u(D_S) = \min \left\{ \text{AR}^u(\mathcal{P}, \mathcal{N}) \mid D_S(\mathcal{P}, \mathcal{N}) = D_S \right\} \quad (7)$$

and

$$\text{AR}_{\max}^u(D_S) = \max \left\{ \text{AR}^u(\mathcal{P}, \mathcal{N}) \mid D_S(\mathcal{P}, \mathcal{N}) = D_S \right\}. \quad (8)$$

In these equations,  $D_S(\mathcal{P}, \mathcal{N}) = 1 - J(\mathcal{P}||\mathcal{N})$  denotes the overlapping ratio between positive and negative samples, with  $J(\mathcal{P}||\mathcal{N})$  being the Jensen-Shannon divergence [40] between the normalized distributions  $\mathcal{P}$  and  $\mathcal{N}$ . At the extremes,  $D_S = 1$  signifies complete overlap, whereas  $D_S = 0$  indicates complete separation.

By employing numerical simulations and heuristic methods (see *SI Appendix, Overlapping and Boundary* for details), we deduce the optimal solutions for these optimization problems as  $\text{AR}_{\min}^u$  and  $\text{AR}_{\max}^u$ . Fig. 3A illustrates a monotonic decrease in both  $\text{AR}_{\min}^u$  and  $\text{AR}_{\max}^u$  as  $D_S$  increases, with the upper bounds for all four datasets analyzed resting between these values. This suggests that greater overlap between positive and negative samples correlates with a reduction in the achievable upper bound for binary classification performance. In the limit, the upper bound can attain 1 (perfect accuracy) when  $D_S = 0$ , and 0.5 (equivalent to random guessing) when  $D_S = 1$ .

### Effect of Feature Selection.

The influence of feature selection on the upper bound is scrutinized. Fig. 3B presents a case study utilizing the AID dataset. It is observed that the upper bound tends to rise with the inclusion of additional features. Nevertheless, there exists a specific subset of features—the optimal feature subset—that is adequate to reach the potential upper bound for the majority of datasets. Beyond this subset, incorporating more features does not enhance the upper bound. It is also noted that integrating transformations of features from the optimal subset fails to provide any further increase in the upper bound. Collectively, these insights underscore the efficacy of our



methodology in streamlining the binary classification process by pinpointing the most effective subset of features for feature engineering purposes.

## Conclusion and Discussion

This research delves into the impact that characteristics of features have on the upper limit of predictive accuracy in binary classification endeavors. Through a combination of theoretical analysis and numerical experimentation, we have shed light on the pivotal roles played by data distribution and feature selection in determining the ceiling of a model’s performance. Additionally, we introduce a quantitative assessment of error balance ( $\Delta$ ), which offers insights into the practicality of reaching these upper bounds in both training and testing scenarios.

The implications of our findings for machine learning (ML) are substantial. We have empirically confirmed that datasets with greater overlap among samples pose more significant challenges for accurate classification. Our theoretical framework convincingly demonstrates that expanding the feature set can reduce overlap between classes and push the boundaries of predictive performance higher. Therefore, in the context of raw data, the discovery and curation of new features, along with the strategic selection of an optimal subset, are crucial for maximizing the efficacy of model training. On the other hand, relying solely on transformations of existing features does not contribute to an improvement of the upper performance limit.

Nonetheless, our study has limitations. Firstly, the theoretical upper bound of prediction performance is attainable only in an ideal scenario where all distinct samples are correctly classified, which does not account for the balance between data availability and model complexity. In real-world applications, achieving this upper bound is often challenging due to constraints on data and computational resources. The degree to which the upper bound can be approached is contingent upon the data distribution, and a theoretical framework to quantify this degree is an avenue for future investigation. Secondly, our analysis presumes that the data space is discretized. The practical utility of the derived upper bound would benefit from considering the distance and similarity between data samples, which we have not addressed. We advocate for future studies that explore the implications of limited model complexity and the behavior in a continuous data space.

Expanding beyond the realm of binary classification, the principles of our boundary theory could also enhance our comprehension of multiclass classification issues, which can be segmented into a series of binary classification challenges. Looking ahead, our forthcoming endeavors will concentrate on the predictability and interpretability within a more applied framework,

particularly concerning feature engineering, given classifiers, optimization techniques, and energy landscapes. In subsequent research, we aim to advance the predictability of ML and AI systems, enhancing the trustworthiness of AI by improving our ability to explain, manage, and regulate these systems.

## Methods & Materials

### Objective Functions.

**Square Loss.** It is denoted based on the square error between the predicted class and actual label for every instance dataset [41], reads

$$\min_g \frac{1}{m} \sum_{x_i} (g(x_i) - y_i)^2.$$

Its corresponding optimal classifier must satisfy,

$$g_{\text{Square}}^*(x_i) = p_+(x_i) - p_-(x_i), \quad (9)$$

for every  $x_i \in \mathcal{S}$ .

**Logistic Loss.** The Logistic loss is defined as [42],

$$\min_g \frac{1}{m} \sum_{x_i} -y_i \log g(x_i) - (1 - y_i) \log (1 - g(x_i))$$

Its corresponding optimal classifier must satisfy,

$$g_{\text{Logistic}}^*(x_i) = p_+(x_i) - p_-(x_i), \quad (10)$$

for every  $x_i \in \mathcal{S}$ .

**Hinge Loss.** Hinge loss aims to maximize the margin between the decision boundary and data points [43], reads

$$\min_g \frac{1}{2m} \sum_{x_i} \max \{0, 1 - g(x_i)y_i\}.$$

Its corresponding optimal classifier must satisfy,

$$g_{\text{Hinge}}^*(x_i) = \begin{cases} 1 & \mathcal{P}(x_i) \geq \mathcal{N}(x_i) \\ -1 & \mathcal{P}(x_i) < \mathcal{N}(x_i), \end{cases} \quad (11)$$

for every  $x_i \in \mathcal{S}$ .

**Softmax Loss.** Assume that  $f(x_i)$  is the probability that data with feature vector  $x_i$  belongs to positive class [44], reads

$$\min_g \frac{1}{m} \sum_{x_i} -\log g(x_i) - \log(1 - g(x_i)).$$

Its corresponding optimal classifier must satisfy,

$$g_{\text{Softmax}}^*(x_i) = p_+(x_i), \quad (12)$$

for every  $x_i \in \mathcal{S}$ .

The mathematical details for these optimal classifiers (Eqs. 9-12) of corresponding objective functions can be found in *SI Appendix, Objective Functions*.

## Acknowledge

This work was supported by the National Natural Science Foundation of China (Grant Nos. 72371224 and 71972164), the Major Project of The National Social Science Fund of China (Grant No. 19ZDA324), the Research Grants Council of the Hong Kong Special Administrative Region (Grant No. 11218221) and the Fundamental Research Funds for the Central Universities.

- 
- [1] T. Hastie, R. Tibshirani, J. H. Friedman, and J. H. Friedman, *The elements of statistical learning: data mining, inference, and prediction*, vol. 2 (Springer, 2009).
  - [2] A. Agresti, *Categorical data analysis*, vol. 792 (John Wiley & Sons, 2012).
  - [3] W. S. Noble, *Nature Biotechnology* **24**, 1565 (2006).
  - [4] T. Chen and C. Guestrin, in *Proceedings of the 22nd acm sigkdd international conference on knowledge discovery and data mining* (2016), pp. 785–794.
  - [5] L. Rosasco, E. De Vito, A. Caponnetto, M. Piana, and A. Verri, *Neural Computation* **16**, 1063 (2004).
  - [6] C. Cortes and M. Mohri, *Advances in neural information processing systems* **16** (2003).
  - [7] T. Yang and Y. Ying, *ACM Computing Surveys* **55**, 1 (2022).
  - [8] T. Joachims, in *Proceedings of the 22nd international conference on Machine learning* (2005), pp. 377–384.
  - [9] Y. Ying, L. Wen, and S. Lyu, *Advances in neural information processing systems* **29** (2016).
  - [10] M. Norton and S. Uryasev, *Mathematical Programming* **174**, 575 (2019).

- [11] Z. Yuan, Y. Yan, M. Sonka, and T. Yang, in *Proceedings of the IEEE/CVF International Conference on Computer Vision* (2021), pp. 3040–3049.
- [12] W. Gao and Z.-H. Zhou, in *International Joint Conference on Artificial Intelligence* (2012), URL <https://api.semanticscholar.org/CorpusID:11266780>.
- [13] Y. Lei, A. Ledent, and M. Kloft, *Advances in Neural Information Processing Systems* **33**, 21236 (2020).
- [14] T. Fawcett, *Pattern Recognition Letters* **27**, 861 (2006).
- [15] J. Sun, L. Feng, J. Xie, X. Ma, D. Wang, and Y. Hu, *Nature communications* **11**, 574 (2020).
- [16] L. Lü, L. Pan, T. Zhou, Y.-C. Zhang, and H. E. Stanley, *Proceedings of the National Academy of Sciences* **112**, 2325 (2015).
- [17] M. Majnik and Z. Bosnić, *Intelligent data analysis* **17**, 531 (2013).
- [18] C. E. Metz, in *Seminars in nuclear medicine* (Elsevier, 1978), vol. 8, pp. 283–298.
- [19] T. Fawcett, in *Proceedings 2001 IEEE International Conference on Data Mining* (2001), pp. 131–138.
- [20] N. Bohr et al., *The quantum postulate and the recent development of atomic theory*, vol. 3 (Printed in Great Britain by R. & R. Clarke, Limited, 1928).
- [21] S. Menard, *Applied logistic regression analysis*, 106 (Sage, 2002).
- [22] D. W. Hosmer Jr, S. Lemeshow, and R. X. Sturdivant, *Applied logistic regression*, vol. 398 (John Wiley & Sons, 2013).
- [23] S. Haykin, *Neural networks: a comprehensive foundation* (Prentice Hall PTR, 1998).
- [24] S. Albawi, T. A. Mohammed, and S. Al-Zawi, in *2017 International Conference on Engineering and Technology (ICET)* (2017), pp. 1–6.
- [25] M. P. Brown, W. N. Grundy, D. Lin, N. Cristianini, C. W. Sugnet, T. S. Furey, M. Ares Jr, and D. Haussler, *Proceedings of the National Academy of Sciences* **97**, 262 (2000).
- [26] C. Kingsford and S. L. Salzberg, *Nature Biotechnology* **26**, 1011 (2008).
- [27] S. Safavian and D. Landgrebe, *IEEE Transactions on Systems, Man, and Cybernetics* **21**, 660 (1991).
- [28] J. A. Hanley and B. J. McNeil, *Radiology* **143**, 29 (1982).
- [29] A. P. Bradley, *Pattern Recognition* **30**, 1145 (1997).
- [30] N. H. Tran, X. Zhang, L. Xin, B. Shan, and M. Li, *Proceedings of the National Academy of Sciences* **114**, 8247 (2017).
- [31] R. G. Congalton, *Remote Sensing of Environment* **37**, 35 (1991).
- [32] A. Madani, R. Arnaout, M. Mofrad, and R. Arnaout, *NPJ Digital Medicine* **1**, 6 (2018).

- [33] S.-C. Kim, A. S. Arun, M. E. Ahsen, R. Vogel, and G. Stolovitzky, *Proceedings of the National Academy of Sciences* **118**, e2100761118 (2021).
- [34] Y. Liu, H. Zhao, J. Gu, Y. Qiao, and C. Dong, *IEEE Transactions on Pattern Analysis and Machine Intelligence* pp. 1–16 (2023).
- [35] J. Xu, Y. Y. Tang, B. Zou, Z. Xu, L. Li, Y. Lu, and B. Zhang, *IEEE Transactions on Cybernetics* **45**, 1169 (2015).
- [36] P. L. Bartlett, P. M. Long, G. Lugosi, and A. Tsigler, *Proceedings of the National Academy of Sciences* **117**, 30063 (2020).
- [37] Y. Jiang, D. Krishnan, H. Mobahi, and S. Bengio, in *International Conference on Learning Representations* (2019), URL <https://openreview.net/forum?id=HJlQfnCqKX>.
- [38] X. Ying, in *Journal of Physics: Conference Series* (IOP Publishing, 2019), vol. 1168, p. 022022.
- [39] N. Srivastava, G. Hinton, A. Krizhevsky, I. Sutskever, and R. Salakhutdinov, *The journal of machine learning research* **15**, 1929 (2014).
- [40] M. Menéndez, J. Pardo, L. Pardo, and M. Pardo, *Journal of the Franklin Institute* **334**, 307 (1997).
- [41] K. P. Körding and D. M. Wolpert, *Proceedings of the National Academy of Sciences* **101**, 9839 (2004).
- [42] A. Ahmed and E. P. Xing, *Proceedings of the National Academy of Sciences* **106**, 11878 (2009).
- [43] G. Xu, Z. Cao, B.-G. Hu, and J. C. Principe, *Pattern Recognition* **63**, 139 (2017).
- [44] F. Wang, J. Cheng, W. Liu, and H. Liu, *IEEE Signal Processing Letters* **25**, 926 (2018).

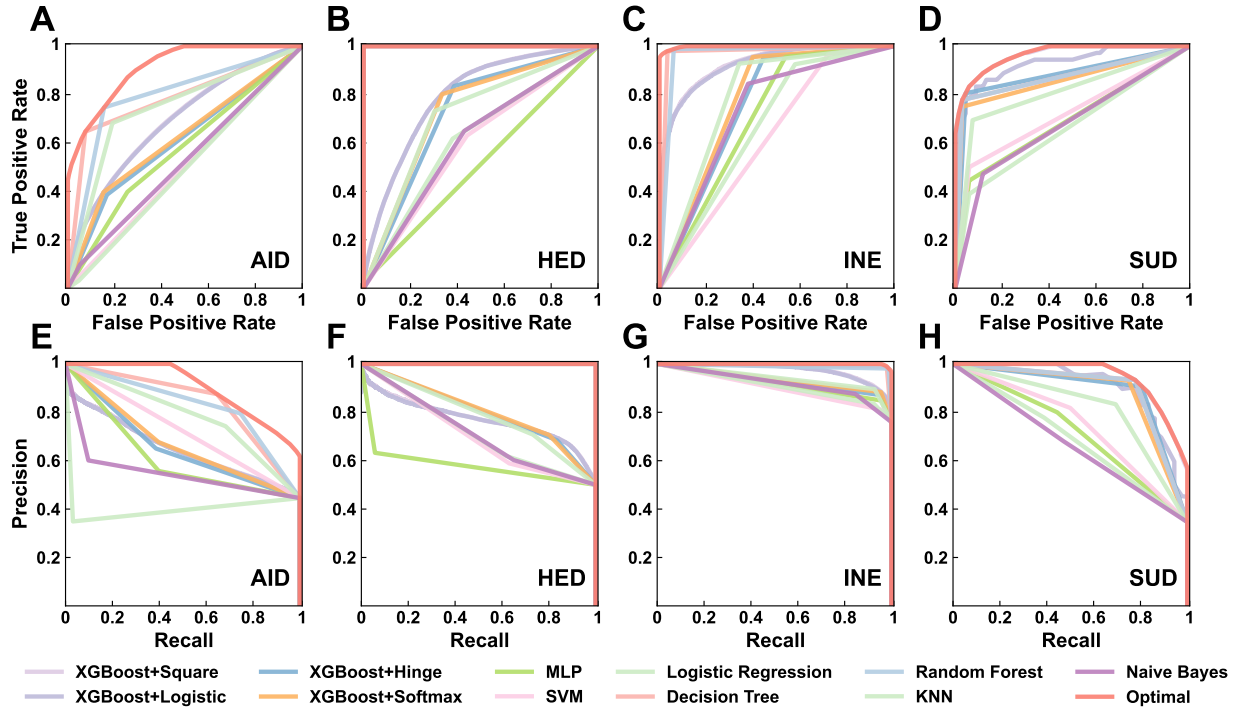


Fig. 1: Demonstrating the precise upper Bound of AUC with accompanying optimal ROC curves (A-D) and PR curves (E-H) across four real-world datasets utilizing a suite of binary classifiers. The classifiers include XGBoost, MLP, SVM, Logistic Regression, Decision Tree, Random Forest, KNN, and Naive Bayes. The red curves symbolize the theoretical optimal PR curves. Detailed values for each classifier-dataset combination are documented in Table 1.

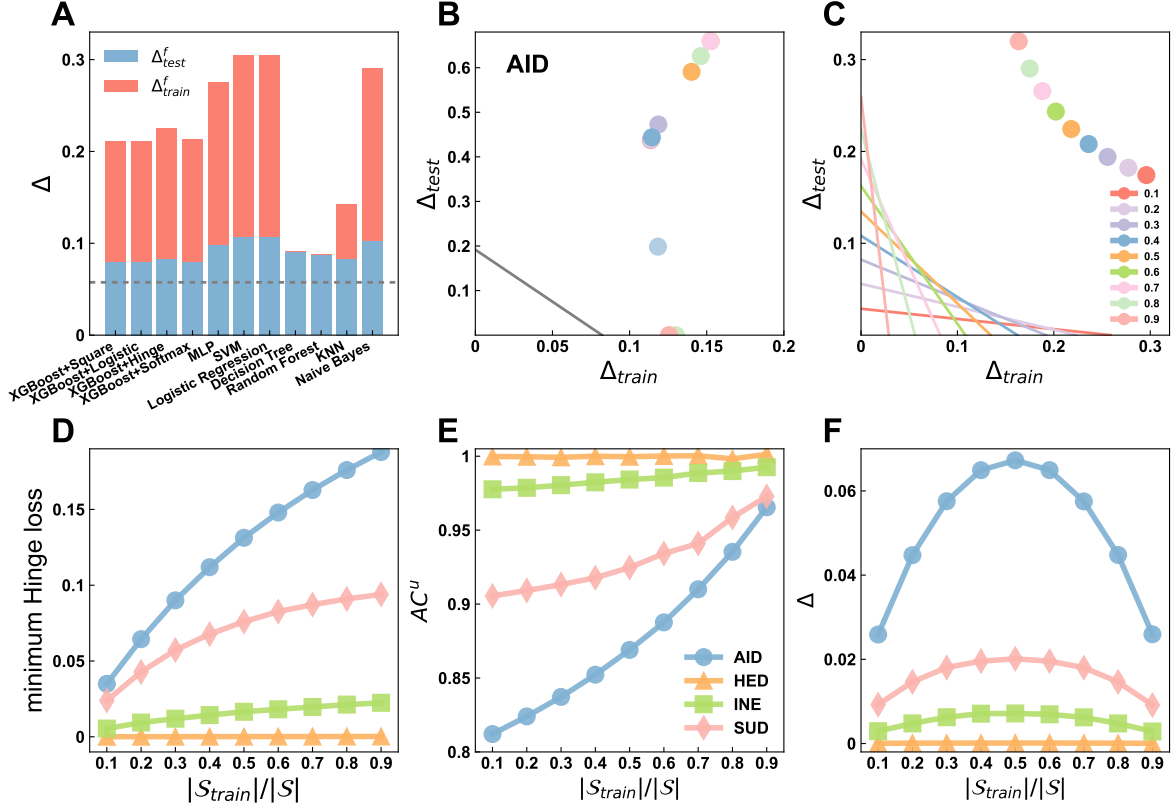


Fig. 2: Detailed evaluation of expected errors ( $\Delta$ ) across all feature vectors for each dataset. Panels A and B showcase the error dynamics for the AID dataset during training ( $\Delta_{train}^f$ ) and testing ( $\Delta_{test}^f$ ) phases, considering a random division ratio where the training set size  $|S_{train}|$  constitutes 70% of the total set size  $|S|$ . (A) The dashed line indicates the expected error of the optimal classifier as determined by Eq. 5. (B) Illustrates the correlation between  $\Delta_{train}^f$  and  $\Delta_{test}^f$ , contrasting the theoretical solution outlined in Eq. 5 (gray line) against empirical observations from diverse binary classifiers (represented by dots). (C) Explores the interplay between  $\Delta_{train}^f$  and  $\Delta_{test}^f$  under a spectrum of random division ratios  $|S_{train}|/|S|$ , varying from 10% to 90%. (D-F) depict the expected errors or performance metrics for each dataset under different random divisions: (D) Hinge loss, (E) upper bound of accuracy ( $AC^u$ ), and (F) anticipated optimal errors ( $\Delta$ ). In these panels, dots correspond to numerical results derived from the data divisions, while lines represent the theoretical predictions adjusted for the respective division ratios (as detailed in Eqs. 54 and 56 within the *SI Appendix, Random Division*).

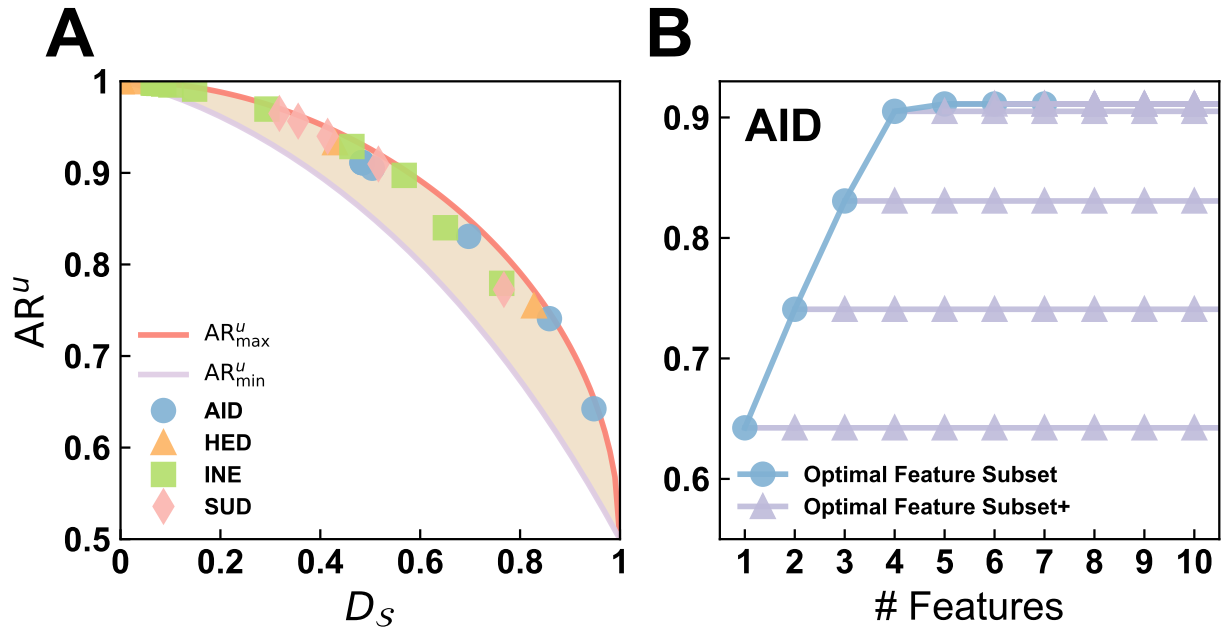


Fig. 3: Characterization of the upper bound for AUC-ROC ( $AR^u$ ) as influenced by key dataset properties on the *AID* dataset, with extended results for additional datasets available in the *SI Appendix, Fig. S6*. (A) Illustrates how  $AR^u$  varies with the degree of overlap ( $D_S$ ) between positive and negative sample distributions. The red and purple curves denote the theoretically expected maximum and minimum bounds, respectively. The plotted dots represent the empirically obtained optimal AUC scores corresponding to different overlapping scenarios facilitated by feature selection. (B) Depicts the relationship between  $AR^u$  and the number of features, where the blue curve indicates the maximum upper bounds achievable with a specified number of features within the *optimal feature subset*. The purple curves denote the maximal upper bounds achievable when the *optimal feature subset* is expanded by the inclusion of additional arbitrary feature transformations, referred to as the *optimal feature subset+*.



Table 1: Comprehensive experimental results and theoretical upper bound analysis for various binary classifiers on four real datasets. The classifiers evaluated include XGBoost, Multilayer Perceptron (MLP), Support Vector Machine (SVM), Logistic Regression (LR), Decision Tree (DT), Random Forest (RF), K-Nearest Neighbors (KNN), and Naive Bayes (NB). Performance metrics for each classifier are presented in terms of area under the ROC curve (AUC-ROC, abbreviated as AR), area under the Precision-Recall curve (AUC-PR, abbreviated as AP), and Accuracy (AC).

Data	Metrics	XGBoost				MLP	SVM	LR	DT	RF	KNN	NB	Boundaries
		Square	Logistic	Hinge	Softmax								
AID	AR	0.6941	0.6917	0.6096	0.6223	0.5777	0.5	0.4921	0.7863	0.7961	0.7464	0.5228	0.9112
	AP	0.6517	0.6491	0.5245	0.5373	0.4939	0.4454	0.4424	0.7232	0.7065	0.6483	0.4606	0.8806
	AC	0.6491	0.6476	0.634	0.6469	0.5957	0.5546	0.5546	0.8015	0.8015	0.7533	0.5692	0.8015
HED	AR	0.7959	0.7948	0.7249	0.7337	0.6127	0.595	0.619	0.9998	0.9997	0.7149	0.6103	1.0
	AP	0.7702	0.769	0.6541	0.6652	0.5767	0.5562	0.574	0.9998	0.9996	0.6523	0.5667	1.0
	AC	0.7349	0.7347	0.7249	0.7337	0.6126	0.595	0.619	0.9998	0.9997	0.7149	0.6103	0.9998
INE	AR	0.9275	0.9239	0.7543	0.7788	0.7467	0.6229	0.6737	0.9728	0.9638	0.794	0.7336	0.9983
	AP	0.9751	0.9738	0.8659	0.8778	0.8627	0.8071	0.829	0.9844	0.9783	0.886	0.8577	0.9993
	AC	0.8734	0.8699	0.857	0.8704	0.839	0.8008	0.8043	0.9764	0.9764	0.8635	0.7913	0.9764
SUD	AR	0.9645	0.9322	0.8807	0.8603	0.6855	0.7206	0.665	0.8742	0.8807	0.8105	0.6773	0.9649
	AP	0.9396	0.9031	0.7973	0.7848	0.5309	0.5822	0.514	0.8028	0.7973	0.6845	0.5038	0.9381
	AC	0.9038	0.8942	0.9038	0.8942	0.7596	0.7885	0.75	0.9038	0.9038	0.8462	0.7404	0.9038

# Contents

<b>Supplementary Note 1: Preliminaries</b>	<b>2</b>
<b>Supplementary Note 2: Objective Functions</b>	<b>3</b>
Square Loss Function . . . . .	3
Logistic Loss Function . . . . .	4
Hinge Loss Function . . . . .	5
Softmax Loss Function . . . . .	5
<b>Supplementary Note 3: Evaluation Measurements</b>	<b>6</b>
Optimal ROC Curve . . . . .	6
Optimal PR Curve . . . . .	9
Optimal Accuracy . . . . .	11
<b>Supplementary Note 4: Sensitivity Analysis</b>	<b>12</b>
<b>Supplementary Note 5: Random Division</b>	<b>13</b>
<b>Supplementary Note 6: Overlapping and Boundary</b>	<b>15</b>
<b>Supplementary Note 7: Feature Engineering</b>	<b>18</b>
Feature Selection . . . . .	20
Feature Extraction . . . . .	22
<b>Supplementary Note 8: Datasets</b>	<b>22</b>
<b>Supplementary Note 9: Supplementary Figures</b>	<b>23</b>

## Supplementary Note 1: Preliminaries

Binary classification involves assigning elements of a set into one of two groups, or classes, based on a classification rule. This process is crucial in various applications such as medical diagnostics, quality control, and information retrieval. In machine learning and data analysis, binary classification is a supervised learning task aimed at predicting one of two possible outcomes for a given input.

In this context, the data is labeled as positive (often denoted by 1) or negative (denoted by -1). The objective is to construct a predictive model capable of accurately classifying new, unseen instances into these categories by learning from patterns in the training data. Initially, a labeled dataset is gathered, where each instance is associated with a known class label. The dataset is then divided into a training set for model development and a test set for evaluating performance on new data. During training, the model identifies patterns that distinguish between the classes. Techniques such as XGBoost, MLP, SVM, LR, DT, RF, KNN, and Naive Bayes can be utilized for binary classification.

Let's consider a binary classification scenario where the goal is to predict a binary label. An input-output pair is represented as  $z = (x, y)$ , where  $x \in \mathcal{X}$  is the feature vector (input data) and  $y \in \{1, -1\}$  is the class label. Given a training set  $\mathcal{S} = \{(x_i, y_i) | i = 1, 2, \dots, m\}$ , we define  $\mathcal{S}_+$  as the subset containing  $n_+$  positive samples and  $\mathcal{S}_-$  as the subset with  $n_-$  negative samples, such that the total number of instances is  $m = |\mathcal{S}| = n_+ + n_-$ . Let  $\mathcal{P}(x_i)$  and  $\mathcal{N}(x_i)$  denote the counts of positive and negative instances for a given feature vector  $x_i$ .

Classifiers are mappings that assign instances to specific classes. Some produce a continuous output, allowing various thresholds to define class membership—these are known as **\*\*continuous classifiers\*\***. They combine a classification function  $f(x) : \mathcal{X} \rightarrow \mathbb{R}$  with a threshold  $t$  to translate scores into binary classes. Others yield a discrete class label—these are **\*\*discrete classifiers\*\*** and are described by the function  $f(x) : \mathcal{X} \rightarrow \{1, -1\}$ . Logistic regression and neural networks are examples of continuous classifiers, while SVM, decision trees, and random forests are discrete classifiers.

Objective functions gauge the alignment between model predictions and actual labels. During training, the aim is to minimize the difference between these predictions and true labels. We discuss several objective functions for binary classification problems:

- Square loss function:  $\min_f \frac{1}{m} \sum_{x_i} (f(x_i) - y_i)^2$ ;
- Logistic loss function:  $\min_f \frac{1}{m} \sum_{x_i} -y_i \log f(x_i) - (1 - y_i) \log (1 - f(x_i))$ ;
- Hinge loss function:  $\min_f \frac{1}{2m} \sum_{x_i} \max \{0, 1 - f(x_i)y_i\}$ ;

- Softmax function:  $\min_f \frac{1}{m} \sum_{x_i} -\log f(x_i) - \log(1 - f(x_i))$ .

Square and Logistic loss functions are typically suited for continuous classifiers, while Hinge and Softmax losses can be applied to both continuous and discrete classifiers.

For binary classification outcomes, we consider the instances to be either positive or negative, leading to four potential results from the classifier:

- TP (True Positive):  $\sum_{x_i \in \mathcal{S}} \frac{P(x_i)}{2} (f(x_i) + 1)$ ;
- FP (False Positive):  $\sum_{x_i \in \mathcal{S}} \frac{N(x_i)}{2} (f(x_i) + 1)$ ;
- FN (False Negative):  $\sum_{x_i \in \mathcal{S}} \frac{P(x_i)}{2} (1 - f(x_i))$ ;
- TN (True Negative):  $\sum_{x_i \in \mathcal{S}} \frac{N(x_i)}{2} (1 - f(x_i))$ .

## Supplementary Note 2: Objective Functions

The objective function in the training process of a classification model serves as a guide for parameter adjustment to fit the dataset. Here, we discuss four commonly used objective functions and show a direct correlation between their optimal solutions [?] and the dataset through discrete analysis.

### Square Loss Function

Given a dataset  $\mathcal{S}$  with feature domain  $\mathcal{X}$ , and assuming  $f(x)$  as a continuous classification function with parameters to be trained, the square error loss function is given by:

$$\min_f \frac{1}{m} \sum_{x_i} (f(x_i) - y_i)^2. \quad (1)$$

The optimal solution for this objective function is expressed as:

$$f_{\text{Square}}^* = \arg \min_f \frac{1}{m} \sum_{x_i} (f(x_i) - y_i)^2. \quad (2)$$

It's evident that:

$$\min_f \sum_{x_i} (f(x_i) - y_i)^2 \geq \sum_{x_i} \min_{f(x_i)} (f(x_i) - y_i)^2. \quad (3)$$

Moreover, equality holds:

$$\min_f \sum_{x_i} (f(x_i) - y_i)^2 = \sum_{x_i} \min_{f(x_i)} (f(x_i) - y_i)^2. \quad (4)$$

if and only if  $f(x_i)$  and  $f(x_j)$  are nearly independent for any  $x_i \neq x_j \in \mathcal{S}$ . In the binary classification context, the square loss function can be transformed to:

$$\begin{aligned} \min_f \sum_{x_i} \left( f(x_i) - y_i \right)^2 &= \sum_{x_i} \min_{f(x_i)} \left( f(x_i) - y_i \right)^2 \\ &= \sum_{x_i} \min_{f(x_i)} \mathcal{P}(x_i) \left( f(x_i) - 1 \right)^2 + \mathcal{N}(x_i) \left( f(x_i) + 1 \right)^2. \end{aligned} \quad (5)$$

The optimal solution becomes:

$$f_{\text{Square}}^*(x_i) = \arg \min_{f(x_i)} \mathcal{P}(x_i) \left( f(x_i) - 1 \right)^2 + \mathcal{N}(x_i) \left( f(x_i) + 1 \right)^2 \quad (6)$$

and is simply:

$$f_{\text{Square}}^*(x_i) = \frac{\mathcal{P}(x_i) - \mathcal{N}(x_i)}{\mathcal{P}(x_i) + \mathcal{N}(x_i)} \quad (7)$$

for each  $x_i \in \mathcal{S}$ .

## Logistic Loss Function

The Logistic loss function, frequently used for binary classification, is defined for a dataset  $\mathcal{S}$  and feature domain  $\mathcal{X}$  as:

$$\min_f \frac{1}{m} \sum_{x_i} -y_i \log f(x_i) - (1 - y_i) \log (1 - f(x_i)), \quad (8)$$

with the optimal solution:

$$f_{\text{Logistic}}^* = \arg \min_f \frac{1}{m} \sum_{x_i} -y_i \log f(x_i) - (1 - y_i) \log (1 - f(x_i)). \quad (9)$$

Close to the optimal, the logistic loss function can be approximated as:

$$\min_f \frac{1}{m} \sum_{x_i} \left( \mathcal{N}(x) - \mathcal{P}(x) \right) \log f(x) - 2\mathcal{N}(x) \log (1 - f(x)). \quad (10)$$

The corresponding optimal solution then is:

$$f_{\text{Logistic}}^*(x_i) = \arg \min_{f(x_i)} \left( \mathcal{N}(x_i) - \mathcal{P}(x_i) \right) \log f(x_i) - 2\mathcal{N}(x_i) \log (1 - f(x_i)) \quad (11)$$

for each  $x_i \in \mathcal{S}$ . Finally, it can be simplified as

$$f_{\text{Logistic}}^*(x_i) = \frac{\mathcal{P}(x_i) - \mathcal{N}(x_i)}{\mathcal{P}(x_i) + \mathcal{N}(x_i)} \quad (12)$$

for each  $x_i \in \mathcal{S}$ .

## Hinge Loss Function

The hinge loss function is commonly used in Support Vector Machines (SVM) and other models employing maximum-margin classifiers, regardless of whether the classification task is discrete or continuous. It penalizes misclassified instances based on their distance from the decision boundary. The Hinge loss function for binary classification is described as follows:

$$\min_f \frac{1}{m} \sum_{i=1}^m \max\{0, 1 - y_i f(x_i)\}, \quad (13)$$

and its optimal solution is

$$f_{\text{Hinge}}^* = \arg \min_f \frac{1}{m} \sum_{i=1}^m \max\{0, 1 - y_i f(x_i)\}. \quad (14)$$

Unlike other objective functions, the output for any solution of the hinge loss function is discrete. We employ a similar technique to the hinge loss function as before,

$$\max_{f(x_i) \in \{1, -1\}} \mathcal{P}(x_i) \max\{0, 1 - f(x_i)\} + \mathcal{N}(x_i) \max\{0, 1 + f(x_i)\} \quad (15)$$

for any  $x_i$ , where its optimal solution can also be expressed as

$$f_{\text{Hinge}}^*(x_i) = \arg \max_{f(x_i) \in \{1, -1\}} \mathcal{P}(x_i) \max\{0, 1 - f(x_i)\} + \mathcal{N}(x_i) \max\{0, 1 + f(x_i)\} \quad (16)$$

for each  $x_i \in \mathcal{S}$ . Since  $f(x_i)$  must be equal to 1 or  $-1$ , we can rewrite the optimal solution as

$$f_{\text{Hinge}}^*(x_i) = \begin{cases} 1, & \text{if } \mathcal{P}(x_i) \geq \mathcal{N}(x_i), \\ -1, & \text{if } \mathcal{P}(x_i) < \mathcal{N}(x_i), \end{cases} \quad (17)$$

for each  $x_i \in \mathcal{S}$ .

## Softmax Loss Function

The Softmax loss function, also known as the cross-entropy loss or log-likelihood loss, is essential in machine learning and deep learning, particularly for classification tasks. It measures the dissimilarity between predicted class probabilities and true class labels. The softmax function is typically used in conjunction with this loss function to convert raw model outputs into probability distributions over multiple classes. Mathematically, for a feature  $x$ , the softmax function computes the probability of the positive class as follows:

$$f(x) = \frac{e^{z_+}}{e^{z_+} + e^{z_-}}. \quad (18)$$

Here,  $z_+$  ( $z_-$ ) denotes the score that measures the likelihood of the data with feature  $x$  belonging to the positive (negative) class.

The softmax loss function is defined as the negative log-likelihood of the true class in binary classification tasks:

$$\min_f \frac{1}{m} \sum_{i=1}^m [-y_i \log f(x_i) - (1 - y_i) \log(1 - f(x_i))], \quad (19)$$

with the optimal solution being

$$f_{\text{Softmax}}^* = \arg \min_f \frac{1}{m} \sum_{i=1}^m [-y_i \log f(x_i) - (1 - y_i) \log(1 - f(x_i))]. \quad (20)$$

We can simplify the objective function as

$$\min_{f(x_i)} -\mathcal{P}(x_i) \log f(x_i) - \mathcal{N}(x_i) \log(1 - f(x_i)), \quad (21)$$

and its optimal solution as

$$f_{\text{Softmax}}^*(x_i) = \arg \min_{f(x_i)} -\mathcal{P}(x_i) \log f(x_i) - \mathcal{N}(x_i) \log(1 - f(x_i)), \quad (22)$$

for every  $x_i \in \mathcal{S}$ . By performing the necessary derivations, we find the optimal solution for the Softmax loss function as

$$f_{\text{Softmax}}^*(x_i) = \frac{\mathcal{P}(x_i)}{\mathcal{P}(x_i) + \mathcal{N}(x_i)}, \quad (23)$$

for each  $x_i \in \mathcal{S}$ .

## Supplementary Note 3: Evaluation Measurements

The evaluation of the performance of binary classifiers involves various metrics, among which the Receiver Operating Characteristic (ROC) curve and the Precision-Recall (PR) curve are prominent. These metrics offer insights into the effectiveness of a classifier at different threshold settings. This note delves into the optimal ROC and PR curves [?, ?], providing a mathematical exposition of their derivation and interpretation in the context of a given dataset.

### Optimal ROC Curve

The ROC curve represents the trade-off between the true positive rate (TPR) and the false positive rate (FPR) of a classifier. The curve is constructed by plotting TPR against FPR at various threshold levels. An optimal ROC curve approaches the top-left corner of the plot, indicating both high TPR and low FPR.

Consider a dataset  $\mathcal{S} = \{x_1, x_2, \dots, x_m\}$  with a feature domain  $\mathcal{X}$ . A classifier  $f$  assigns a score to each instance in  $\mathcal{S}$ , resulting in a sorted sequence  $\mathcal{S}^f = \{x_1^f, x_2^f, \dots, x_n^f\}$ , where  $f(x_i^f) \geq f(x_j^f)$  for  $i < j$ . The real label corresponding to  $x_i^f$  is denoted as  $y_i^f$ . To construct the ROC curve, one must calculate the TPR and FPR at various thresholds  $t \in \{1, \dots, m\}$  where each  $t = k$  indicates that instances  $x_1^f, \dots, x_k^f$  are classified as positive. The TPR and FPR are given by:

$$\text{TPR} = \frac{\text{TP}}{n_+} = \frac{1}{n_+} \sum_{i=1}^k \frac{1}{2} (1 + y_i^f), \quad (24)$$

$$\text{FPR} = \frac{\text{FP}}{n_-} = \frac{1}{n_-} \sum_{i=1}^k \frac{1}{2} (1 - y_i^f). \quad (25)$$

To find the optimal ROC curve, the objective is to maximize TPR and minimize FPR for each threshold  $k$ . This bi-objective optimization can be expressed as:

$$\begin{aligned} \max_f \quad & \sum_{i=1}^k \frac{1}{2} (1 + y_i^f), \\ \min_f \quad & \sum_{i=1}^k \frac{1}{2} (1 - y_i^f). \end{aligned} \quad (26)$$

Considering that the sum of true positives and false positives equals  $k$ , the optimization problem in Eq. (26) simplifies to:

$$\max \quad \sum_{i=1}^k \frac{1}{2} (1 + y_i^f). \quad (27)$$

The calculation of FPR for a fixed  $k$  includes instances that either exceed or equal the score  $f(x_k^f)$ . However, the optimization is primarily concerned with the maximization of true positives. Therefore we have

$$\sum_{i=1}^k \frac{1}{2} (1 + y_i^f) = \sum_{i=1}^m \frac{1}{2} \mathbb{1}(f(x_i) > f(x_k^f)) (1 + y_i) + \frac{\alpha}{2} \mathbb{1}(f(x_i) = f(x_k^f)) (1 + y_i), \quad (28)$$

in which  $\alpha = \frac{k - \sum_{i=1}^m \mathbb{1}(f(x_i) > f(x_k^f))}{\sum_{i=1}^m \mathbb{1}(f(x_i) = f(x_k^f))}$  is the ratio of instances with score  $f(x_k^f)$  in the subset  $\{x_1^f, x_2^f, \dots, x_k^f\}$  to all instances with score  $f(x_k^f)$ . Without loss of generality, we assume that  $f(x_i) = f(x_j) \iff x_i =$



$x_j$  for every  $x_i, x_j \in \mathcal{S}$ . Then we obtain that

$$\begin{aligned}
& \sum_{i=1}^k \frac{1}{2} (1 + y_i^f) \\
&= \sum_{x_i \in \mathcal{S}} \mathbb{I}(f(x_i) > f(x_k^f)) \mathcal{P}(x_i) + \alpha \sum_{x_i \in \mathcal{S}} \mathbb{I}(f(x_i) = f(x_k^f)) \mathcal{P}(x_i) \\
&= \sum_{i=1}^m \mathbb{I}(f(x_i) > f(x_k^f)) \frac{\mathcal{P}(x_i)}{\mathcal{P}(x_i) + \mathcal{N}(x_i)} + \alpha \sum_{i=1}^m \mathbb{I}(f(x_i) = f(x_k^f)) \frac{\mathcal{P}(x_k^f)}{\mathcal{P}(x_k^f) + \mathcal{N}(x_k^f)} \quad (29) \\
&= \sum_{i=1}^m \mathbb{I}(f(x_i) > f(x_k^f)) \frac{\mathcal{P}(x_i)}{\mathcal{P}(x_i) + \mathcal{N}(x_i)} + \left( k - \sum_{i=1}^m \mathbb{I}(f(x_i) > f(x_k^f)) \right) \frac{\mathcal{P}(x_k^f)}{\mathcal{P}(x_k^f) + \mathcal{N}(x_k^f)} \\
&= \sum_{i=1}^m \frac{\mathcal{P}(x_i^f)}{\mathcal{P}(x_i^f) + \mathcal{N}(x_i^f)}.
\end{aligned}$$

Denote  $w_i = \frac{\mathcal{P}(x_i)}{\mathcal{P}(x_i) + \mathcal{N}(x_i)}$  as the non-negative weight of instance  $x_i$ . Hence, the optimization problem (27) can be regarded as a problem of how to choose a  $k$ -elements subset of  $\mathcal{S}$  which satisfies that the total weight is maximum. And it is naturally rewritten in the form of combinatorial optimization as follows,

$$\begin{aligned}
& \max \quad \sum_{i=1}^m w_i z_i \\
& \text{s.t.} \quad \sum_{i=1}^m z_i = k \\
& \quad \quad z_i \in \{0, 1\}, \quad i = 1, 2, \dots, m
\end{aligned} \quad (30)$$

Actually, this combinatorial optimization problem belongs to the classical 0-1 knapsack problems, which is the most common problem being solved. Noting that all weights are non-negative, simple greedy algorithm can reach the optimal solution if we select the top  $k$  instances with the highest weight. As a rule of how to select optimal  $k$ -element subset with arbitrary  $k$ , the optimal classifier for best ROC curve is the weight function, that is,

$$f_{\text{ROC}}^*(x_i) = \frac{\mathcal{P}(x)}{\mathcal{P}(x_i) + \mathcal{N}(x_i)} \quad (31)$$

for every  $x_i \in \mathcal{S}$ . Here, we denote that  $\{x_1^*, x_2^*, \dots, x_n^*\}$  is the sorted sequence of  $\mathcal{S}$  in descending order of weight.

Naturally, the best ROC curve can be drawn sequentially from a series of data points in (FPR, TPR)-plane as follows,

$$\left\{ \left( \frac{1}{n_-} \sum_{i=1}^k \frac{\mathcal{N}(x_i^*)}{\mathcal{P}(x_i^*) + \mathcal{N}(x_i^*)}, \frac{1}{n_+} \sum_{i=1}^k \frac{\mathcal{P}(x_i^*)}{\mathcal{P}(x_i^*) + \mathcal{N}(x_i^*)} \right) \right\}_{k=0,1,\dots,n} \quad (32)$$

The optimal ROC curve can be regarded as a combination of  $n$  linear piecewise functions, whose derivatives are composed of the following sequence

$$\left\{ \frac{n_- \mathcal{P}(x_i^*)}{n_+ \mathcal{N}(x_i^*)} \right\}_{k=1,2,\dots,n}. \quad (33)$$

It is easy to check that, the above sequence is monotonically decreasing, since  $\{x_1^*, x_2^*, \dots, x_n^*\}$  is sorted by descending order of weight and

$$\frac{\mathcal{P}(x_i^*)}{\mathcal{P}(x_i^*) + \mathcal{N}(x_i^*)} = \frac{1}{1 + \frac{1}{\frac{\mathcal{P}(x_i^*)}{\mathcal{N}(x_i^*)}}}. \quad (34)$$

Therefore, the best ROC curve is **concave**. Moreover, the area under the best ROC curve is the upper bound of AR ( $\text{textAR}^u$ ). In other words,  $\text{AR}^u$  is equal to the area under the curve described as  $f_{\text{ROC}}^*$  in the following:

$$\begin{aligned} \text{AR}^u &= \sum_{i=1}^m \frac{1}{n_-} \frac{\mathcal{N}(x_i^*)}{\mathcal{P}(x_i^*) + \mathcal{N}(x_i^*)} \left( \frac{1}{n_+} \sum_{j < i} \frac{\mathcal{P}(x_j^*)}{\mathcal{P}(x_j^*) + \mathcal{N}(x_j^*)} + \frac{1}{2n_+} \frac{\mathcal{P}(x_i^*)}{\mathcal{P}(x_i^*) + \mathcal{N}(x_i^*)} \right) \\ &= \frac{1}{n_- n_+} \sum_{i > j} \frac{\mathcal{N}(x_i^*) \mathcal{P}(x_j^*)}{\left( \mathcal{P}(x_i^*) + \mathcal{N}(x_i^*) \right) \left( \mathcal{P}(x_j^*) + \mathcal{N}(x_j^*) \right)} + \frac{1}{2} \sum_{i=1}^m \frac{\mathcal{N}(x_i^*) \mathcal{P}(x_i^*)}{\left( \mathcal{P}(x_i^*) + \mathcal{N}(x_i^*) \right)^2} \\ &= \frac{1}{2n_- n_+} \sum_{i,j} \frac{\max \left\{ \mathcal{N}(x_i^*) \mathcal{P}(x_j^*), \mathcal{N}(x_j^*) \mathcal{P}(x_i^*) \right\}}{\left( \mathcal{P}(x_i^*) + \mathcal{N}(x_i^*) \right) \left( \mathcal{P}(x_j^*) + \mathcal{N}(x_j^*) \right)} \\ &= \frac{1}{2n_- n_+} \sum_{i,j} \frac{\max \left\{ \mathcal{N}(x_i) \mathcal{P}(x_j), \mathcal{N}(x_j) \mathcal{P}(x_i) \right\}}{\left( \mathcal{P}(x_i) + \mathcal{N}(x_i) \right) \left( \mathcal{P}(x_j) + \mathcal{N}(x_j) \right)} \\ &= \frac{1}{2n_- n_+} \sum_{x_i, x_j} \max \left\{ \mathcal{P}(x_i) \mathcal{N}(x_j), \mathcal{P}(x_j) \mathcal{N}(x_i) \right\}. \end{aligned} \quad (35)$$

### Optimal PR Curve

The precision-recall (PR) curve is a widely utilized metric for evaluating binary classifiers, emphasizing the trade-off between precision and recall. It provides a detailed view of a classifier's performance at various decision thresholds. To plot a PR curve, one must compute precision and recall at numerous thresholds. This concept is analogous to the receiver operating characteristic (ROC) curve, which allows adjustment of the threshold to balance precision and recall.

For each threshold value, precision and recall are determined using the following formulas:

$$\text{precision} = \frac{\text{TP}}{\text{TP} + \text{FP}}, \quad (36)$$

where TP is the number of true positives and FP is the number of false positives. Recall, also known as true positive rate (TPR), is defined as:

$$\text{recall} = \frac{\text{TP}}{\text{TP} + \text{FN}}, \quad (37)$$

where FN is the number of false negatives. Both the ROC and PR curves share a commonality in that they evaluate the classifier's performance by computing metrics at various thresholds. At a specific threshold  $k$ , the precision and recall can be expressed as:

$$\text{precision} = \frac{\text{TP}}{k} = \frac{n_+}{k} \times \text{TPR}, \quad (38)$$

$$\text{recall} = \text{TPR}, \quad (39)$$

where  $n_+$  is the total number of positive samples.

The objective in seeking the optimal PR curve is to maximize both precision and recall for a given threshold  $k$ . This can be formulated as the following optimization problem:

$$\max_f \text{TPR}, \quad (40)$$

which we have addressed in the previous section. The optimal classifier that achieves the best PR curve is identical to the one that optimizes the ROC curve and is given by:

$$f_{\text{PR}}^*(x) = f_{\text{ROC}}^*(x) = \frac{\mathcal{P}(x)}{\mathcal{P}(x) + \mathcal{N}(x)}, \quad (41)$$

where  $x$  belongs to the sample space  $\mathcal{S}$ . The optimal PR curve is constructed by plotting a series of data points in the (recall, precision)-plane, which are calculated as follows:

$$\left\{ \left( \frac{1}{n_+} \sum_{i=1}^k \frac{\mathcal{P}(x_i^*)}{\mathcal{P}(x_i^*) + \mathcal{N}(x_i^*)}, \frac{1}{k} \sum_{i=1}^k \frac{\mathcal{P}(x_i^*)}{\mathcal{P}(x_i^*) + \mathcal{N}(x_i^*)} \right) \right\}_{k=0,1,\dots,n} \quad (42)$$

Furthermore, the upper bound of the area under the PR curve ( $\text{AP}^u$ ) can be calculated as follows:

$$\text{AP}^u = \frac{1}{2n_+} \sum_{x_i^*} p_+(x_i^*) \left( \frac{1}{i-1} \sum_{j=1}^{i-1} p_+(x_j^*) + \frac{1}{i} \sum_{j=1}^i p_+(x_j^*) \right), \quad (43)$$

where  $p_+(x_i)$  is the probability of a sample  $x_i$  being positive:

$$p_+(x_i) = \frac{\mathcal{P}(x_i)}{\mathcal{P}(x_i) + \mathcal{N}(x_i)}. \quad (44)$$

## Optimal Accuracy

Accuracy (AC) is a fundamental metric that quantifies the proportion of correctly predicted instances against the total number of instances within a dataset. This metric is universally applicable across classifiers. Given a dataset  $\mathcal{S}$  and a feature space  $\mathcal{X}$ , accuracy can be computed with the following expression:

$$\text{AC} = \frac{1}{2m} \sum_{x_i \in \mathcal{S}} (1 + f(x_i)y_i), \quad (45)$$

where  $m$  represents the total number of instances,  $f(x_i)$  is the predicted label for instance  $x_i$ , and  $y_i$  is the true label. The accuracy increases by  $\frac{1}{2m}$  for each correctly classified instance  $x_i$ ; it remains unchanged for incorrect predictions.

While accuracy itself is not a conventional loss function, optimizing for the highest possible accuracy and determining the optimal classifier functions are critical endeavors in machine learning. The mathematical upper limit of accuracy, denoted as  $\text{AC}^u$ , can be formalized as:

$$\text{AC}^u = \max_f \frac{1}{2m} \sum_{x_i \in \mathcal{S}} (1 + f(x_i)y_i), \quad (46)$$

with the corresponding optimal classifier being:

$$f_{\text{AC}}^* = \arg \max_f \frac{1}{2m} \sum_{x_i \in \mathcal{S}} (1 + f(x_i)y_i). \quad (47)$$

Through further analysis, we can expand and simplify the equation by considering the relationship between probabilities associated with positive and negative instances:

$$\begin{aligned} \max_f \sum_{x_i \in \mathcal{S}} \frac{1}{2m} (1 + f(x_i)y_i) &= \max_f \sum_{x \in \mathcal{X}} \frac{\mathcal{P}(x)}{2} (1 + f(x)) + \frac{\mathcal{N}(x)}{2} (1 - f(x)) \\ &\leq \sum_{x_i \in \mathcal{S}} \max_{f(x)} \frac{\mathcal{P}(x_i)}{2} (1 + f(x_i)) + \frac{\mathcal{N}(x_i)}{2} (1 - f(x_i)), \end{aligned} \quad (48)$$

which leads us to redefine  $\text{AC}^u$  as:

$$\text{AC}^u = \max_{f(x_i)} \frac{\mathcal{P}(x_i)}{2} (1 + f(x_i)) + \frac{\mathcal{N}(x_i)}{2} (1 - f(x_i)), \quad (49)$$

and the optimal classifier for each instance  $x_i \in \mathcal{S}$  becomes:

$$f_{\text{AC}}^*(x_i) = \arg \max_{f(x_i)} \frac{\mathcal{P}(x_i)}{2} (1 + f(x_i)) + \frac{\mathcal{N}(x_i)}{2} (1 - f(x_i)). \quad (50)$$

By enumeration, the solution for the optimal classifier is:

$$f_{\text{AC}}^*(x_i) = \begin{cases} 1 & \text{if } \mathcal{P}(x_i) \geq \mathcal{N}(x_i), \\ -1 & \text{if } \mathcal{P}(x_i) < \mathcal{N}(x_i), \end{cases} \quad (51)$$

resulting in the upper limit of accuracy being:

$$\text{AC}^u = \frac{1}{m} \sum_{x_i \in \mathcal{S}} \max \{ \mathcal{P}(x_i), \mathcal{N}(x_i) \}. \quad (52)$$

## Supplementary Note 4: Sensitivity Analysis

In Supplementary Notes 2 and 3, we established the mathematical relationships between the lower bound of the objective function with respect to the training set and the upper bound of the evaluation metrics related to the test set. This section extends that discussion within the out-of-sample framework by combining these relationships to investigate the dual concerns of training loss and generalizability in classification tasks.

Let us denote the training and test sets by  $\mathcal{S}_{train}$  and  $\mathcal{S}_{test}$ , respectively. Furthermore, we denote  $\mathcal{P}_{train}(x_i)$  and  $\mathcal{N}_{train}(x_i)$  as the respective counts of positive and negative instances with feature  $x_i$  in the training set, and similarly,  $\mathcal{P}_{test}(x_i)$  and  $\mathcal{N}_{test}(x_i)$  for the test set.

For a discrete classifier  $f(x)$ , the boundary hinge loss within the training set  $\mathcal{S}_{train}$  is defined as:

$$\sum_{x_i} \min\{\mathcal{P}_{train}(x_i), \mathcal{N}_{train}(x_i)\}. \quad (53)$$

Here,  $\Delta_{train}$  represents the discrepancy between the classifier's hinge loss and the boundary hinge loss, expressed as:

$$\Delta_{train} = \sum_{x_i} \Delta_{train}(x_i),$$

where

$$\Delta_{train}(x_i) = \begin{cases} \mathcal{N}_{train}(x_i) - \min\{\mathcal{P}_{train}(x_i), \mathcal{N}_{train}(x_i)\} & \text{if } f(x_i) = 1, \\ \mathcal{P}_{train}(x_i) - \min\{\mathcal{P}_{train}(x_i), \mathcal{N}_{train}(x_i)\} & \text{if } f(x_i) = -1. \end{cases}$$

In parallel, the maximum accuracy achievable on the test set  $\mathcal{S}_{test}$  is:

$$\sum_{x_i} \max\{\mathcal{P}_{test}(x_i), \mathcal{N}_{test}(x_i)\}.$$

Similarly,  $\Delta_{test}$  quantifies the error between the classifier's actual accuracy and the maximum possible accuracy:

$$\Delta_{test} = \sum_{x_i} \Delta_{test}(x_i),$$

where

$$\Delta_{test}(x_i) = \begin{cases} \max\{\mathcal{P}_{test}(x_i), \mathcal{N}_{test}(x_i)\} - \mathcal{P}_{test}(x_i) & \text{if } f(x_i) = 1, \\ \max\{\mathcal{P}_{test}(x_i), \mathcal{N}_{test}(x_i)\} - \mathcal{N}_{test}(x_i) & \text{if } f(x_i) = -1. \end{cases}$$

Therefore, the summation of these two discrepancies represents their respective optimization poten-

tial and performance evaluation capacity. For any given feature  $x_i$ , the combined error is:

$$(\Delta_{train} + \Delta_{test})(x_i) = \begin{cases} \mathcal{N}_{train}(x_i) - \min\{\mathcal{P}_{train}(x_i), \mathcal{N}_{train}(x_i)\} + \max\{\mathcal{P}_{test}(x_i), \mathcal{N}_{test}(x_i)\} - \mathcal{P}_{test}(x_i) & \text{if } f(x_i) = 1, \\ \mathcal{P}_{train}(x_i) - \min\{\mathcal{P}_{train}(x_i), \mathcal{N}_{train}(x_i)\} + \max\{\mathcal{P}_{test}(x_i), \mathcal{N}_{test}(x_i)\} - \mathcal{N}_{test}(x_i) & \text{if } f(x_i) = -1. \end{cases}$$

We now introduce a lower bound for  $(\Delta_{train} + \Delta_{test})$ , defined as:

$$\Delta = (\Delta_{train} + \Delta_{test})_{\min} = \sum_{x_i} \Delta(x_i), \quad (54)$$

where

$$\Delta(x_i) = \min\{\mathcal{N}_{train}(x_i) - \mathcal{P}_{test}(x_i), \mathcal{P}_{train}(x_i) - \mathcal{N}_{test}(x_i)\} + \max\{\mathcal{P}_{test}(x_i), \mathcal{N}_{test}(x_i)\} - \min\{\mathcal{P}_{train}(x_i), \mathcal{N}_{train}(x_i)\}. \quad (55)$$

As we observed,  $\Delta$  is a general lower bound for the sum of training error and evaluation error regardless of the specific classifier in use. Furthermore,  $\Delta = 0$  if and only if

$$\begin{cases} \mathcal{P}_{train}(x_i) \geq \mathcal{N}_{train}(x_i) \\ \mathcal{P}_{test}(x_i) \geq \mathcal{N}_{test}(x_i) \end{cases} \quad \text{or} \quad \begin{cases} \mathcal{N}_{train}(x_i) \geq \mathcal{P}_{train}(x_i) \\ \mathcal{N}_{test}(x_i) \geq \mathcal{P}_{test}(x_i) \end{cases}$$

for each  $x_i \in \mathcal{S}$ .

## Supplementary Note 5: Random Division

*Random division* method is a standard approach to splitting a dataset into training and testing subsets. In this method, each instance is independently assigned to the training subset with probability  $p$  and to the testing subset with probability  $1 - p$ . For a given feature vector  $x_i$ , the counts  $\mathcal{P}_{train}(x_i)$  and  $\mathcal{N}_{train}(x_i)$  follow binomial distributions  $\mathcal{B}(\mathcal{P}(x_i), p)$  and  $\mathcal{B}(\mathcal{N}(x_i), p)$  respectively. Considering this, we can investigate the discrepancy  $\Delta$  within the context of probabilistic partitioning. We define the expected value of  $\Delta$  as  $\mathbb{E}[\Delta] = \frac{1}{m} \sum_{x_i} \mathbb{E}[\Delta(x_i; p)]$ , which is calculated as:

$$\begin{aligned} \mathbb{E}[\Delta(x_i; p)] &= \mathbb{E}[\min\{\mathcal{N}_{train}(x_i) - \mathcal{P}_{test}(x_i), \mathcal{P}_{train}(x_i) - \mathcal{N}_{test}(x_i)\}] + \\ &\quad \mathbb{E}[\max\{\mathcal{P}_{test}(x_i), \mathcal{N}_{test}(x_i)\}] - \mathbb{E}[\min\{\mathcal{P}_{train}(x_i), \mathcal{N}_{train}(x_i)\}] \\ &= \mathbb{E}[\max\{\mathcal{P}_{test}(x_i), \mathcal{N}_{test}(x_i)\}] + \mathbb{E}[\max\{\mathcal{P}_{train}(x_i), \mathcal{N}_{train}(x_i)\}] - \\ &\quad \max\{\mathcal{P}(x_i), \mathcal{N}(x_i)\}, \end{aligned} \quad (56)$$

where the expected maxima are determined by:

$$\mathbb{E}[\max\{\mathcal{P}_{train}(x_i), \mathcal{N}_{train}(x_i)\}] = \sum_{i=0}^{\mathcal{P}(x_i)} \sum_{j=0}^{\mathcal{N}(x_i)} \max\{i, j\} \binom{\mathcal{P}(x_i)}{i} \binom{\mathcal{N}(x_i)}{j} p^{\mathcal{P}(x_i)+\mathcal{N}(x_i)-i-j} (1-p)^{i+j},$$

and

$$\mathbb{E}[\max\{\mathcal{P}_{test}(x_i), \mathcal{N}_{test}(x_i)\}] = \sum_{i=0}^{\mathcal{P}(x_i)} \sum_{j=0}^{\mathcal{N}(x_i)} \max\{i, j\} \binom{\mathcal{P}(x_i)}{i} \binom{\mathcal{N}(x_i)}{j} p^{i+j} (1-p)^{\mathcal{P}(x_i)+\mathcal{N}(x_i)-i-j}.$$

It's important to note that  $\Delta$  is symmetric; its value is invariant if we exchange the roles of the training and testing subsets  $\mathcal{S}_{train}$  and  $\mathcal{S}_{test}$ . This symmetry is apparent in the equality  $\mathbb{E}[\Delta(x_i; p)] = \mathbb{E}[\Delta(x_i; 1-p)]$ , as both expressions yield the same result.

We observe that  $\Delta$  exhibits symmetrical behavior, as its value remains invariant under the interchange of the training set  $\mathcal{S}_{train}$  and the test set  $\mathcal{S}_{test}$ . This symmetry property is further substantiated by the equality in expected values for complementary probabilities in the random partitioning process, expressed mathematically as  $\mathbb{E}[\Delta(x_i; p)]$ .

To enhance the interpretability of experimental outcomes, we derive mathematical representations for two key metrics: the expected maximum accuracy of the test set, denoted as  $AC^u$ , and the expected minimum hinge loss for the training set. These metrics, in the context of random partitioning, are defined by the following equations:

- For the expected maximum accuracy of the test set:

$$\mathbb{E}AC^u = \frac{1}{m(1-p)} \sum_{x_i} \mathbb{E} \max\{\mathcal{P}_{test}(x_i), \mathcal{N}_{test}(x_i)\} \quad (57)$$

- For the expected minimum hinge loss of the training set:

$$\mathbb{E}[\text{minimum hinge loss}] = \frac{1}{mp} \sum_{x_i} \mathbb{E} \min\{\mathcal{P}_{train}(x_i), \mathcal{N}_{train}(x_i)\} \quad (58)$$

The expected minimum, present in the equation for hinge loss, is elucidated as follows:

$$\mathbb{E}[\min\{\mathcal{P}_{train}(x_i), \mathcal{N}_{train}(x_i)\}] = \sum_{i=0}^{\mathcal{P}(x_i)} \sum_{j=0}^{\mathcal{N}(x_i)} \min\{i, j\} \binom{\mathcal{P}(x_i)}{i} \binom{\mathcal{N}(x_i)}{j} p^{\mathcal{P}(x_i)+\mathcal{N}(x_i)-i-j} (1-p)^{i+j}. \quad (59)$$

In these expressions,  $\mathcal{P}_{train}(x_i)$  and  $\mathcal{N}_{train}(x_i)$  denote the number of positive and negative instances of  $x_i$  in the training set, respectively, and analogously for  $\mathcal{P}_{test}(x_i)$  and  $\mathcal{N}_{test}(x_i)$  in the test set. The binomial coefficients reflect the combinatorial possibilities for selecting  $i$  positives out of  $\mathcal{P}(x_i)$  and  $j$  negatives out of  $\mathcal{N}(x_i)$ , factoring in the probability  $p$  of an instance belonging to the training set.

## Supplementary Note 6: Overlapping and Boundary

Indeed, training loss and evaluation metrics inherently have a lower bound (0) and an upper bound (1). However, as analyzed in Supplementary Notes 2 and 3, the precise boundaries do not always align with these natural limits. The reason is that positive and negative samples sometimes overlap, making it impossible for any classifier to achieve 100% prediction accuracy. Consequently, this section will further explore the quantifiable correlation between the degree of overlap among positive and negative samples in a dataset and the performance boundaries. However, prior to this exploration, our first step will be to establish a definition for the term ‘‘overlap’’ within the context of a dataset.

Given positive data distribution  $\{\mathcal{P}(x_i)/n_+\}_{x_i \in \mathcal{X}}$  and negative data distribution  $\{\mathcal{N}(x_i)/n_-\}_{x_i \in \mathcal{X}}$ , these two probability distributions can be abbreviated as

$$\mathcal{P} := \{\hat{p}(x_i)|x_i \in \mathcal{S}\}$$

and

$$\mathcal{Q} := \{\hat{n}(x_i)|x_i \in \mathcal{S}\}$$

respectively, in which  $\hat{p}(x_i) = \mathcal{P}(x_i)/n_+$  and  $\hat{n}(x_i) = \mathcal{N}(x_i)/n_-$  for every  $x_i \in \mathcal{S}$ . Considering that Jensen-Shannon divergence is a symmetry and bounded measures to quantify the divergence degree between two probability distributions, we define the overlapping measures between  $\mathcal{P}$  and  $\mathcal{Q}$  as the complement of  $J(\mathcal{P}||\mathcal{N})$ , that is,

$$\begin{aligned} D_{\mathcal{S}} &= 1 - J(\mathcal{P}||\mathcal{N}) \\ &= 1 - \frac{1}{2} \left( \text{KL}(\mathcal{P}||\mathcal{M}) + \text{KL}(\mathcal{N}||\mathcal{M}) \right) \\ &= 1 - \frac{1}{2} \left( \sum_{x_i \in \mathcal{S}} \hat{p}(x_i) \log_2 \left( \frac{2\hat{p}(x_i)}{\hat{p}(x_i) + \hat{n}(x_i)} \right) + \hat{n}(x_i) \log_2 \left( \frac{2\hat{n}(x_i)}{\hat{p}(x_i) + \hat{n}(x_i)} \right) \right) \quad (60) \\ &= -\frac{1}{2} \left( \sum_{x_i \in \mathcal{S}} \hat{p}(x_i) \log_2 \left( \frac{\hat{p}(x_i)}{\hat{p}(x_i) + \hat{n}(x_i)} \right) + \hat{n}(x_i) \log_2 \left( \frac{\hat{n}(x_i)}{\hat{p}(x_i) + \hat{n}(x_i)} \right) \right) \end{aligned}$$

where  $\mathcal{M} = \frac{1}{2}(\mathcal{P} + \mathcal{N})$  is a mixture distribution of  $\mathcal{P}$  and  $\mathcal{N}$ , and  $\text{KL}(\mathcal{P}||\mathcal{N})$  is the Kullback–Leibler divergence of any two distributions  $\mathcal{P}$  and  $\mathcal{N}$ . Here,  $D_{\mathcal{S}}$  is also bounded by zero and one, in particular,  $D_{\mathcal{S}} = 0$  means that they are completely separated;  $D_{\mathcal{S}} = 1$  means that they are totally overlapped. Therefore, the specific value of  $D_{\mathcal{S}} \in [0, 1]$  quantitatively characterizes the degree of overlap between  $\mathcal{P}$  and  $\mathcal{N}$ .

Next, we plan to discover the quantitative relationship between  $D_{\mathcal{S}}$  and  $\text{AR}^u$  through describing the fluctuation of  $\text{AR}^u$  given a fixed overlapping  $D_{\mathcal{S}}$ . At first, we define  $\text{AR}_{\max}^u(D_{\mathcal{S}})$  and  $\text{AR}_{\min}^u(D_{\mathcal{S}})$  as



the maximum and minimum values of upper bound of AUC ( $\text{AR}^u$ ) of dataset  $\mathcal{S}$  with overlapping  $D_{\mathcal{S}}$ , respectively. In other words,  $\text{AR}_{\max}^u(D_{\mathcal{S}})$  and  $\text{AR}_{\min}^u(D_{\mathcal{S}})$  can be obtained through solving the two following optimization problems:

$$\begin{aligned}
& \min \sum_{x_i, x_j \in \mathcal{S}} \max \left\{ \hat{p}(x_i) \hat{n}(x_j), \hat{n}(x_i) \hat{p}(x_j) \right\} \\
& \text{s.t.} \sum_{x_i \in \mathcal{S}} \hat{p}(x_i) \log_2 \left( \frac{\hat{p}(x_i)}{\hat{p}(x_i) + \hat{n}(x_i)} \right) + \hat{n}(x_i) \log_2 \left( \frac{\hat{n}(x_i)}{\hat{p}(x_i) + \hat{n}(x_i)} \right) + 2D_{\mathcal{S}} = 0 \\
& \sum_{x_i \in \mathcal{S}} \hat{p}(x_i) = 1 \\
& \sum_{x_i \in \mathcal{S}} \hat{n}(x_i) = 1 \\
& \hat{p}(x_i) \geq 0 \quad i = 1, 2, \dots, m \\
& \hat{n}(x_i) \geq 0 \quad i = 1, 2, \dots, m
\end{aligned} \tag{61}$$

and

$$\begin{aligned}
& \max \sum_{x_i, x_j \in \mathcal{S}} \max \left\{ \hat{p}(x_i) \hat{n}(x_j), \hat{n}(x_i) \hat{p}(x_j) \right\} \\
& \text{s.t.} \sum_{x_i \in \mathcal{S}} \hat{p}(x_i) \log_2 \left( \frac{\hat{p}(x_i)}{\hat{p}(x_i) + \hat{n}(x_i)} \right) + \hat{n}(x_i) \log_2 \left( \frac{\hat{n}(x_i)}{\hat{p}(x_i) + \hat{n}(x_i)} \right) + 2D_{\mathcal{S}} = 0 \\
& \sum_{x_i \in \mathcal{S}} \hat{p}(x_i) = 1 \\
& \sum_{x_i \in \mathcal{S}} \hat{n}(x_i) = 1 \\
& \hat{p}(x_i) \geq 0 \quad i = 1, 2, \dots, m \\
& \hat{n}(x_i) \geq 0 \quad i = 1, 2, \dots, m
\end{aligned} \tag{62}$$

Now, we observed an interesting phenomenon that both  $\text{AR}^u$  and  $D_{\mathcal{S}}$  remain unchanged if we swap the values of  $(\hat{p}(x_i), \hat{n}(x_i))$  and  $(\hat{p}(x_j), \hat{n}(x_j))$ . Considering the computational process of  $\text{AR}^u$ , we assume that  $\hat{p}(x_1)/\hat{n}(x_1) \leq \hat{p}(x_2)/\hat{n}(x_2) \leq \dots \leq \hat{p}(x_m)/\hat{n}(x_m)$  without loss of generality. Under this assumption, the  $\text{AR}^u$  can be simplified as

$$\text{AR}^u = \sum_{i=1}^m \sum_{j=1}^{i-1} \hat{p}(x_i) \hat{n}(x_j) + \frac{1}{2} \sum_{i=1}^m \hat{p}(x_i) \hat{n}(x_i). \tag{63}$$

Combined with the above assumption and equation, Eq. 61 and Eq. 62 can be rewritten as

$$\begin{aligned}
\min \quad & \sum_{i=1}^m \sum_{j=1}^{i-1} \hat{p}(x_i) \hat{n}(x_j) + \frac{1}{2} \sum_{i=1}^m \hat{p}(x_i) \hat{n}(x_i) \\
\text{s.t.} \quad & \sum_{i=1}^m \hat{p}(x_i) \log_2 \left( \frac{\hat{p}(x_i)}{\hat{p}(x_i) + \hat{n}(x_i)} \right) + \hat{n}(x_i) \log_2 \left( \frac{\hat{n}(x_i)}{\hat{p}(x_i) + \hat{n}(x_i)} \right) + 2D_S = 0 \\
& \hat{p}(x_1)/\hat{n}(x_1) \leq \hat{p}(x_2)/\hat{n}(x_2) \leq \dots \leq \hat{p}(x_m)/\hat{n}(x_m) \\
& \sum_{i=1}^m \hat{p}(x_i) = 1 \\
& \sum_{i=1}^m \hat{n}(x_i) = 1 \\
& \hat{p}(x_i) \geq 0 \quad i = 1, 2, \dots, m \\
& \hat{n}(x_i) \geq 0 \quad i = 1, 2, \dots, m
\end{aligned} \tag{64}$$

and

$$\begin{aligned}
\max \quad & \sum_{i=1}^m \sum_{j=1}^{i-1} \hat{p}(x_i) \hat{n}(x_j) + \frac{1}{2} \sum_{i=1}^m \hat{p}(x_i) \hat{n}(x_i) \\
\text{s.t.} \quad & \sum_{i=1}^m \hat{p}(x_i) \log_2 \left( \frac{\hat{p}(x_i)}{\hat{p}(x_i) + \hat{n}(x_i)} \right) + \hat{n}(x_i) \log_2 \left( \frac{\hat{n}(x_i)}{\hat{p}(x_i) + \hat{n}(x_i)} \right) + 2D_S = 0 \\
& \hat{p}(x_1)/\hat{n}(x_1) \leq \hat{p}(x_2)/\hat{n}(x_2) \leq \dots \leq \hat{p}(x_m)/\hat{n}(x_m) \\
& \sum_{i=1}^m \hat{p}(x_i) = 1 \\
& \sum_{i=1}^m \hat{n}(x_i) = 1 \\
& \hat{p}(x_i) \geq 0 \quad i = 1, 2, \dots, m \\
& \hat{n}(x_i) \geq 0 \quad i = 1, 2, \dots, m
\end{aligned} \tag{65}$$

respectively. According to the symmetry of the ranking assumption

$$\frac{\hat{p}(x_1)}{\hat{n}(x_1)} \leq \frac{\hat{p}(x_2)}{\hat{n}(x_2)} \leq \dots \leq \frac{\hat{p}(x_m)}{\hat{n}(x_m)},$$

it follows that the feasible region is partitioned into  $m!$  pairwise symmetric sub-regions. Within each sub-region, the mathematical formulation of  $\text{AR}_{\max}^u(D_S)$  is invariant and possesses an identical maximum value. Consequently, we can disregard the ranking assumption in Eq. (65) and deduce a simplified

version as follows:

$$\begin{aligned}
\max \quad & \sum_{i=1}^m \sum_{j=1}^{i-1} \hat{p}(x_i) \hat{n}(x_j) + \frac{1}{2} \sum_{i=1}^m \hat{p}(x_i) \hat{n}(x_i), \\
\text{s.t.} \quad & \sum_{i=1}^m \hat{p}(x_i) \log_2 \left( \frac{\hat{p}(x_i)}{\hat{p}(x_i) + \hat{n}(x_i)} \right) + \hat{n}(x_i) \log_2 \left( \frac{\hat{n}(x_i)}{\hat{p}(x_i) + \hat{n}(x_i)} \right) + 2D_S = 0, \\
& \sum_{i=1}^m \hat{p}(x_i) = 1, \\
& \sum_{i=1}^m \hat{n}(x_i) = 1, \\
& \hat{p}(x_i) \geq 0, \quad i = 1, 2, \dots, m, \\
& \hat{n}(x_i) \geq 0, \quad i = 1, 2, \dots, m.
\end{aligned} \tag{66}$$

We employ the SLSQP solver [?] to resolve the optimization problem outlined in (66) and acquire the corresponding numerical solution for  $\text{AR}_{\max}^u$ . In Fig. S8A, the  $\text{AR}^u$  curve versus  $D_S$  is depicted. Each datum point on the curve represents the numerical solution of the optimization problem under specific parameters. Notably, the curve converges swiftly as  $m$  increases, and attains the optimal  $\text{AR}_{\max}^u$  curve when  $m \geq 10$ .

Regarding the  $\text{AR}_{\min}^u$  curve, a heuristic approach is utilized to construct its optimal solution from the feasible region's boundaries. Specifically, we examine a particular case where  $\hat{p}(x_1) = 1 - b$ ,  $\hat{p}(x_2) = b$ ,  $\hat{n}(x_1) = 0$ , and  $\hat{n}(x_2) = 1$ , with  $b$  being a tunable parameter in the interval  $[0, 1]$ . In this scenario, the  $\text{AR}^u$  is expressed as

$$\text{AR}^u = 1 - \frac{b}{2}, \tag{67}$$

and  $D_S$  is given by

$$\begin{aligned}
D_S &= -\frac{1}{2} \left( b \log_2 \frac{b}{b+1} + \log_2 \frac{1}{b+1} \right) \\
&= -\frac{1}{2} (b \log_2 b - (b+1) \log_2 (b+1)).
\end{aligned} \tag{68}$$

Furthermore, the numerical curve of  $\text{AR}_{\min}^u$  obtained through the SLSQP solver aligns closely with this heuristic solution as given in (68), providing partial validation for our heuristic approach (see Fig. S8B).

## Supplementary Note 7: Feature Engineering

In previous sections, we have discussed the boundaries of the objective function and evaluation metrics from the perspective of row data (feature vectors). In fact, column data (features) can also influence the

degree of overlap and boundaries in a dataset through their impact on row data. In feature engineering, there are two classic methods of handling column data: feature selection and feature extraction. The former emphasizes adding or removing new features unrelated to existing ones, and the latter is based on extraction and mapping of original features. In this section, we will discuss these two methods separately. But before that, we need to discuss the simplest case first.

Suppose we have an original dataset  $\mathcal{S} = \{(x_i, y_i) : i = 1, 2, \dots, m\}$  with  $k$  features. This implies that the feature vector  $x_i$  can be expressed as  $x_i = (x_{i,1}, x_{i,2}, \dots, x_{i,k})$ . We also define that there are  $\mathcal{P}(x_i)$  positive instances and  $\mathcal{N}(x_i)$  negative instances with feature vector  $x_i$  in the entire dataset. By introducing a new feature into every instance, we can create a new dataset  $\mathcal{S}'$ . Using feature vector  $x_i$  as an example, these  $\mathcal{P}(x_i) + \mathcal{N}(x_i)$  could be added into different feature values, which are included in  $\{x_i^s = (x_{i,1}, x_{i,2}, \dots, x_{i,k}, x_{i,k+1}^s) : s = 1, 2, \dots, s_i\}$ . For the sake of argument, we illustrate that the original feature vector is split into  $s_i$  pairwise distinct feature vectors after the addition of one row data, satisfying that

$$\begin{cases} \sum_{j=1}^{s_i} \mathcal{P}(x_i^j) = \mathcal{P}(x_i) \\ \sum_{j=1}^{s_i} \mathcal{N}(x_i^j) = \mathcal{N}(x_i) \end{cases}, \quad (69)$$

in which  $s_i$  is defined as the diversity for  $x_i$ . Consequently, we will proceed to prove the following lemma.

**Lemma 1.** *Upon the inclusion of a new feature into the original dataset,  $AR^u$  will either increase or remain constant, while  $D_S$  will either decrease or stay the same. These values will remain unchanged if, and only if, the diversity  $s_i = 1$  for each  $x_i$ .*

*Proof.* The upper bound of AUC in the original dataset  $\mathcal{S}$

$$AR_{original}^u = \frac{1}{2n_-n_+} \sum_{i,j} \max\{\mathcal{P}(x_i)\mathcal{N}(x_j), \mathcal{P}(x_j)\mathcal{N}(x_i)\}, \quad (70)$$

and the new boundary is

$$\begin{aligned} AR_{new}^u &= \frac{1}{2n_-n_+} \sum_{i,j} \sum_{i'=1}^{s_i} \sum_{j'=1}^{s_j} \max\{\mathcal{P}(x_i^{i'})\mathcal{N}(x_j^{j'}), \mathcal{P}(x_j^{j'})\mathcal{N}(x_i^{i'})\} \\ &\geq \frac{1}{2n_-n_+} \sum_{i,j} \max \left\{ \sum_{i'=1}^{s_i} \mathcal{P}(x_i^{i'}) \sum_{j'=1}^{s_j} \mathcal{N}(x_j^{j'}), \sum_{j'=1}^{s_j} \mathcal{P}(x_j^{j'}) \sum_{i'=1}^{s_i} \mathcal{N}(x_i^{i'}) \right\}. \\ &= \frac{1}{2n_-n_+} \sum_{i,j} \max\{\mathcal{P}(x_i)\mathcal{N}(x_j), \mathcal{P}(x_j)\mathcal{N}(x_i)\} \\ &= AR_{original}^u \end{aligned} \quad (71)$$

Similarly, the original  $D_S$  can be written as

$$D_S^{original} = -\frac{1}{2} \left( \sum_{x_i \in \mathcal{S}} \hat{p}(x_i) \log_2 \left( \frac{\hat{p}(x_i)}{\hat{p}(x_i) + \hat{n}(x_i)} \right) + \hat{n}(x_i) \log_2 \left( \frac{\hat{n}(x_i)}{\hat{p}(x_i) + \hat{n}(x_i)} \right) \right) \quad (72)$$

and the new overlapping is

$$\begin{aligned} D_S^{new} &= -\frac{1}{2} \left( \sum_{x_i \in \mathcal{S}} \sum_{i'=1}^{s_i} \hat{p}(x_i^{i'}) \log_2 \left( \frac{\hat{p}(x_i^{i'})}{\hat{p}(x_i^{i'}) + \hat{n}(x_i^{i'})} \right) + \hat{n}(x_i^{i'}) \log_2 \left( \frac{\hat{n}(x_i^{i'})}{\hat{p}(x_i^{i'}) + \hat{n}(x_i^{i'})} \right) \right) \\ &\leq -\frac{1}{2} \left( \sum_{x_i \in \mathcal{S}} \sum_{i'=1}^{s_i} \hat{p}(x_i^{i'}) \log_2 \left( \frac{\sum_{i'=1}^{s_i} \hat{p}(x_i^{i'})}{\sum_{i'=1}^{s_i} \hat{p}(x_i^{i'}) + \hat{n}(x_i^{i'})} \right) + \sum_{i'=1}^{s_i} \hat{n}(x_i^{i'}) \log_2 \left( \frac{\sum_{i'=1}^{s_i} \hat{n}(x_i^{i'})}{\sum_{i'=1}^{s_i} \hat{p}(x_i^{i'}) + \hat{n}(x_i^{i'})} \right) \right) \\ &= -\frac{1}{2} \left( \sum_{x_i \in \mathcal{S}} \hat{p}(x_i) \log_2 \left( \frac{\hat{p}(x_i)}{\hat{p}(x_i) + \hat{n}(x_i)} \right) + \hat{n}(x_i) \log_2 \left( \frac{\hat{n}(x_i)}{\hat{p}(x_i) + \hat{n}(x_i)} \right) \right) \\ &= D_S^{original}. \end{aligned} \quad (73)$$

They are equal to each other if and only if there exists  $i'$  satisfying that  $\hat{p}(x_i^{i'}) = \hat{p}(x_i)$  and  $\hat{n}(x_i^{i'}) = \hat{n}(x_i)$  for every  $x_i$ , i.e.,  $s_i = 1$ .  $\square$

Actually, adding new features will cause the overlapping of the positive and negative samples of the dataset to decrease or remain unchanged, while reducing the original features will cause the overlapping to increase or remain unchanged. The same conclusion is also applicable to the boundaries of various evaluation indicators and loss functions, such as  $AR^u$ ,  $AP^u$  and  $AC^u$ .

## Feature Selection

Feature selection is the process of selecting a subset of relevant features (variables, predictors) for use in model construction. A feature selection algorithm can be seen as the combination of a search technique for proposing new feature subsets, along with an evaluation measure which scores the different feature subsets. The simplest algorithm is to test each possible subset of features finding the one which minimizes the error rate to reach the best performance. Actually, the exponential number of potential subset selection and the huge amount of training cost for any classifier make this process difficult. However, the boundary theory we proposed can better select subset of all features with high performance measured by  $AR$ ,  $AP$  (best ranking) and  $AC$  and low computational cost (time complexity).

Given an integer  $k_0$ , the optimal  $k_0$  feature subset is targeted by  $AR^u$ . This implies that we can directly compute the  $AR^u$  for each feature subset in the entire dataset  $\mathcal{S}$  to assess the data quality and training potential, bypassing the need for a training process. This approach significantly conserves storage

space and computational resources. We denote  $\text{AR}_{k_0}^u$  and  $D_S^{k_0}$  as the optimal  $\text{AR}^u$  and  $D_S$ , respectively, when we traverse all possible  $k_0$  feature subsets. The corresponding feature subset is named by *optimal feature subset*. Based on Lemma 1 and the principle of recursion, it is evident that

**Theorem 1.**  $\text{AR}_{k_0}^u$  exhibits a monotonic non-decreasing trend and  $D_S^{k_0}$  is monotonic non-increasing when  $k_0 \in \{1, 2, \dots, k\}$ . Here,  $k$  represents the total number of features in the entire dataset.

*Proof.* Based on the principle of recursion, we only need to prove that  $\text{AR}_{k_0}^u \leq \text{AR}_{k_0+1}^u$  and  $D_S^{k_0} \geq D_S^{k_0+1}$  for any  $k_0 \in \{1, 2, \dots, k-1\}$ . Assumed that  $\mathcal{F}_{k_0}^* = \{f_1^*, f_2^*, \dots, f_{k_0}^*\}$  is the optimal  $k_0$ -feature subset. Then we construct a new  $k_0 + 1$ -feature subset  $\mathcal{F}_{k_0+1} = \mathcal{F}_{k_0}^* + \{f_i\}$ , in which  $f_i$  is any selected feature not belonging to  $\mathcal{F}_{k_0}^*$ . According to Lemma 1, we know that the  $\text{AR}^u$  of  $\mathcal{F}_{k_0+1}$  is higher than or equal to  $\text{AR}_{k_0}^u$ . At the same time, we also know that the  $\text{AR}^u$  of  $\mathcal{F}_{k_0+1}$  is lower than or equal to  $\text{AR}_{k_0+1}^u$  since the definition of  $\text{AR}_{k_0+1}^u$ . Therefore, we successfully proved that  $\text{AR}_{k_0}^u \leq \text{AR}_{k_0+1}^u$ . In a similar way, we can also prove  $D_S^{k_0} \geq D_S^{k_0+1}$ .  $\square$

Theorem 1 elucidates the direct correlation between the performance bounds and the overlapping index within a given dataset. Specifically, it reveals that an increase in the number of features (raw data) leads to a reduction in the overlap between the positive and negative sample distributions, which in turn enhances the performance boundaries. This insight informs the design of a feature selection algorithm that leverages the overlapping index,  $D_S$ , to ensure the achievement of the highest possible performance upper limit.

Consider a dataset  $\mathcal{S}$  composed of  $k$  features  $\{F_1, F_2, \dots, F_k\}$ . The optimal feature subset of size  $k_0$ , denoted as the subset that minimizes  $D_S$  (or maximizes  $\text{AR}^u$ ), can be defined where  $k_0 = 1, 2, \dots, k$ . However, exhaustively evaluating all  $\binom{k}{k_0}$  possible subsets may be computationally prohibitive for large  $k$ . To address this, approximation techniques like dynamic programming can be employed to devise an efficient approximation algorithm.

For a more practical example, consider the INE dataset with 13 features; it is possible to achieve the dataset's performance boundary using only 8 features, such that  $D_S^8 = D_S$ . This indicates that the remaining five features are, to some extent, superfluous. We thus define the optimal feature selection dimension  $k^*$  as:

$$k^* = \min\{k_0 : D_S^{k_0} = D_S\}. \quad (74)$$

The feature subset corresponding to  $k^*$  is referred to as the *global optimal feature subset*.

## Feature Extraction

Feature extraction is the procedure of deriving features (traits, properties, attributes) from raw data. It is seen as an equivalent transformation that creates new features from the original ones. In previous subsections, we deduced that the boundary of performance is dictated by the data structure. From a mathematical standpoint, feature extraction can be viewed as a mapping of original features (row data). If we incorporate new extracted data into the original dataset, the diversity for each feature vector is 1. In conjunction with Lemma 1, we can state,

**Theorem 2.** *The inclusion of extracted features into the original dataset does not alter the boundary of training loss, evaluation measures, and overlapping.*

*Proof.* Any feature extraction process can be regarded as a mapping from existing feature vectors, so the diversity is 1. Combined with Lemma 1, the boundaries and overlapping should be unchanged.  $\square$

## Supplementary Note 8: Datasets

We utilized four datasets from the Kaggle platform (<https://www.kaggle.com>) in our study. The specifics of these real-world datasets are as follows:

- Airlines Delay Dataset (AID): comprised of 539,383 records across 8 distinct attributes, the objective is to forecast flight delays based on scheduled departure information. Access this dataset at <https://www.kaggle.com/datasets/jimschacko/airlines-dataset-to-predict-a-delay>.
- Heart Disease Dataset (HED): This dataset encompasses a wide range of cardiovascular risk factors, including age, gender, height, weight, blood pressure, cholesterol and glucose levels, smoking status, alcohol intake, physical activity, and presence of cardiovascular diseases, from over 70,000 individuals. It serves as a valuable asset for applying advanced machine learning methods to investigate the link between these factors and cardiovascular health, which could enhance disease understanding and prevention strategies. Access this dataset at <https://www.kaggle.com/datasets/thedevastator/exploring-risk-factors-for-cardiovascular-diseas>.
- Income Classification Dataset (INE): This dataset features variables such as education, employment, and marital status to predict whether an individual earns more than \$50K annually. Access this dataset at <https://www.kaggle.com/datasets/lodetomasi1995/income-classification>.

- Student Sleep Study Dataset (SUD): Originating from a survey-based analysis of US students’ sleep patterns, this dataset utilizes factors like average sleep duration and phone usage time to infer adequate sleep among students. Access this dataset at <https://www.kaggle.com/datasets/mlomuscio/sleepstudypilot/data>.

These datasets are also available for download from “The Boundary Theory of Binary Classification on GitHub” (<https://github.com/Feijing92/The-boundary-theory-of-binary-classification>). Their statistical properties are detailed in Table 1 (referred to as Table S1 in the paper).

**Table S1:** Description of six real datasets we used in this paper. It includes the number of instances ( $m$ ), the number of positive instances ( $n_+$ ), the number of negative instances ( $n_-$ ), the number of features ( $k$ ), the overlapping index ( $D_S$ ) and the optimal feature selection dimension ( $k^*$ ).

Name	$m$	$n_+$	$n_-$	$k$	$D_S$	$k^*$
AID	539383	299119	240264	7	0.4837	5
HED	70000	34979	35021	11	0.0015	5
INE	32561	7841	24720	13	0.0657	12
SUD	104	36	68	5	0.3181	5

## Supplementary Note 9: Supplementary Figures



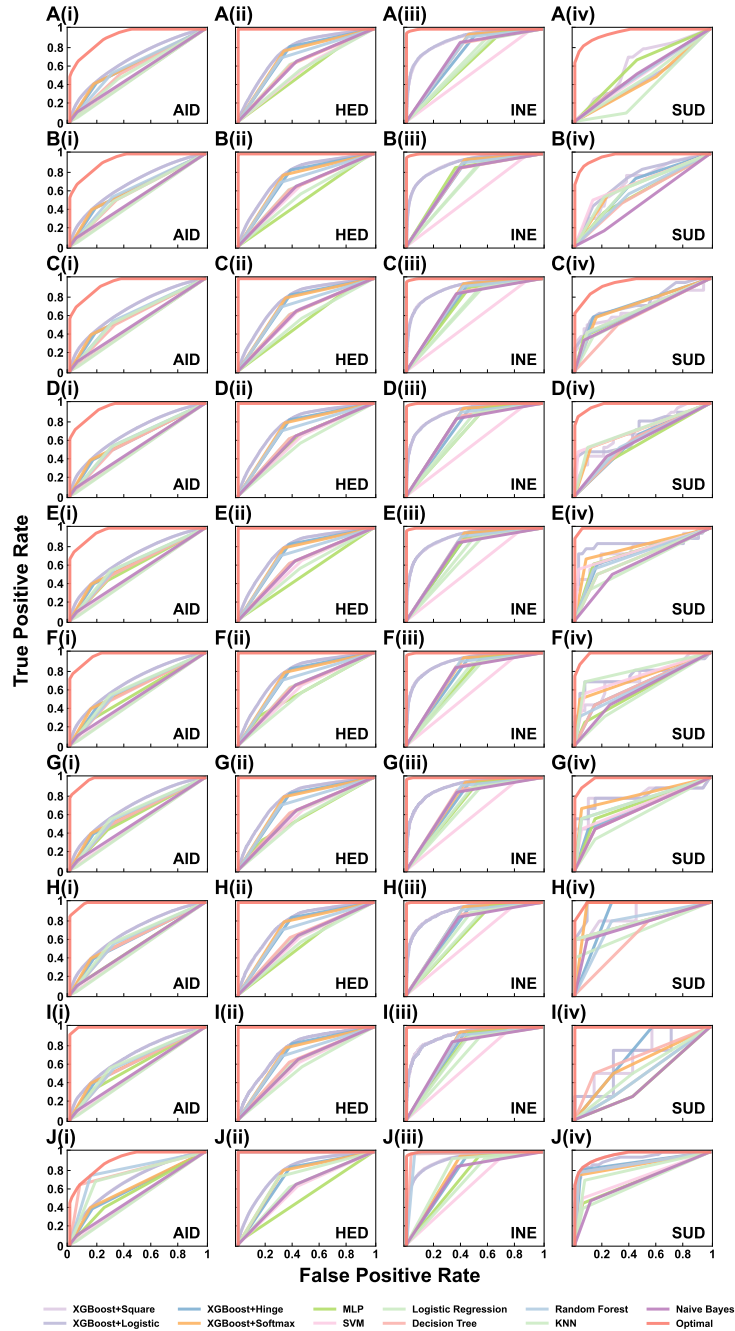


**Fig. S1:** Exact upper bound of AUC and corresponding optimal ROC curves for four real-world datasets when  $|\mathcal{S}_{train}|/|\mathcal{S}| = 0.1$  (A),  $|\mathcal{S}_{train}|/|\mathcal{S}| = 0.2$  (B),  $|\mathcal{S}_{train}|/|\mathcal{S}| = 0.3$  (C),  $|\mathcal{S}_{train}|/|\mathcal{S}| = 0.4$  (D),  $|\mathcal{S}_{train}|/|\mathcal{S}| = 0.5$  (E),  $|\mathcal{S}_{train}|/|\mathcal{S}| = 0.6$  (F),  $|\mathcal{S}_{train}|/|\mathcal{S}| = 0.7$  (G),  $|\mathcal{S}_{train}|/|\mathcal{S}| = 0.8$  (H),  $|\mathcal{S}_{train}|/|\mathcal{S}| = 0.9$  (I),  $|\mathcal{S}_{train}|/|\mathcal{S}| = 1$  (J). The binary classifiers we used in this experiment include XGBoost, MLP, SVM, Logistic Regression, Decision Tree, Random Forest, KNN and Naive Bayes. Red curves represent the theoretical optimal ROC curves.

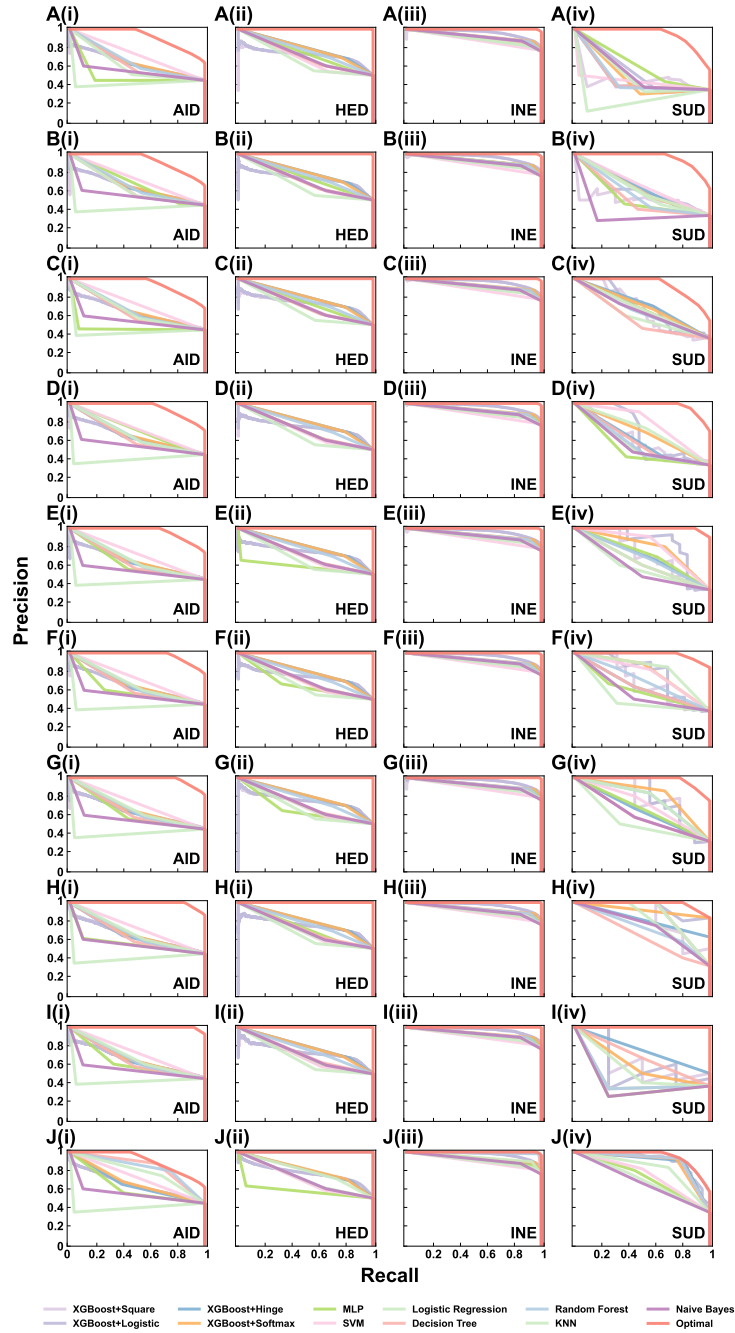


**Fig. S2:** Exact upper bound of AP and corresponding optimal PR curves for four real-world datasets when  $|\mathcal{S}_{train}|/|\mathcal{S}| = 0.1$  (A),  $|\mathcal{S}_{train}|/|\mathcal{S}| = 0.2$  (B),  $|\mathcal{S}_{train}|/|\mathcal{S}| = 0.3$  (C),  $|\mathcal{S}_{train}|/|\mathcal{S}| = 0.4$  (D),  $|\mathcal{S}_{train}|/|\mathcal{S}| = 0.5$  (E),  $|\mathcal{S}_{train}|/|\mathcal{S}| = 0.6$  (F),  $|\mathcal{S}_{train}|/|\mathcal{S}| = 0.7$  (G),  $|\mathcal{S}_{train}|/|\mathcal{S}| = 0.8$  (H),  $|\mathcal{S}_{train}|/|\mathcal{S}| = 0.9$  (I),  $|\mathcal{S}_{train}|/|\mathcal{S}| = 1$  (J). The binary classifiers we used in this experiment include XGBoost, MLP, SVM, Logistic Regression, Decision Tree, Random Forest, KNN and Naive Bayes. Red curves represent the theoretical optimal PR curves.

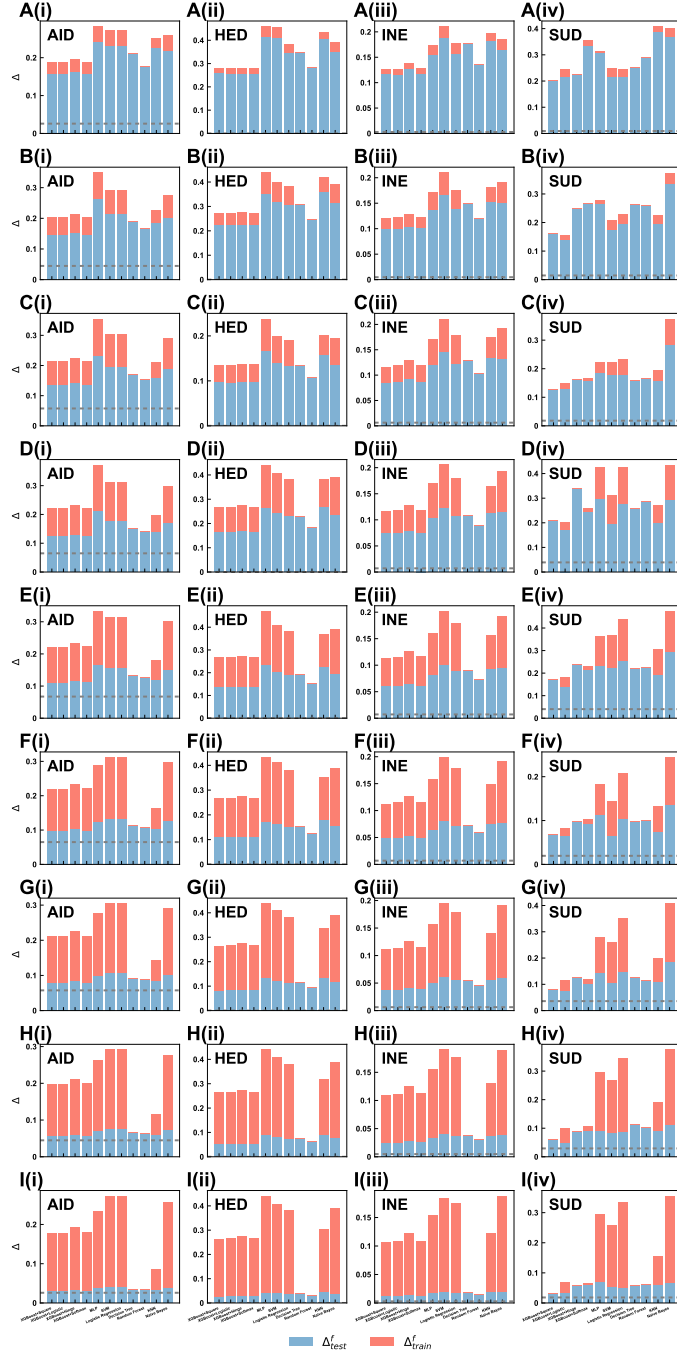


**Fig. S3:** The loss errors of for four datasets in training ( $\Delta_{train}^f$ ) and test sets ( $\Delta_{test}^f$ ) when  $|S_{train}|/|S| = 0.1$  (A),  $|S_{train}|/|S| = 0.2$  (B),  $|S_{train}|/|S| = 0.3$  (C),  $|S_{train}|/|S| = 0.4$  (D),  $|S_{train}|/|S| = 0.5$  (E),  $|S_{train}|/|S| = 0.6$  (F),  $|S_{train}|/|S| = 0.7$  (G),  $|S_{train}|/|S| = 0.8$  (H),  $|S_{train}|/|S| = 0.9$  (I). Dash line represents the expected error of optimal classifier based on Eq. 54.

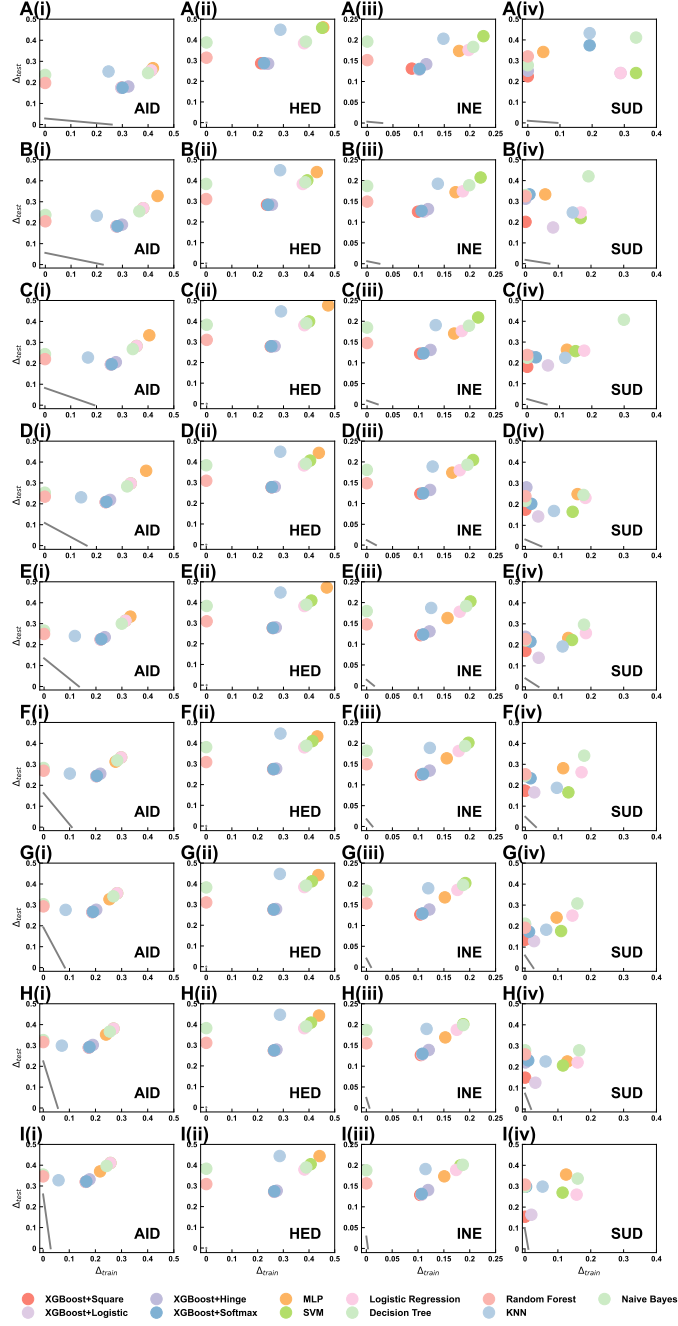


**Fig. S4:** The loss errors of for four datasets in training ( $\Delta_{train}^f$ ) and test sets ( $\Delta_{test}^f$ ) when  $|S_{train}|/|S| = 0.1$  (A),  $|S_{train}|/|S| = 0.2$  (B),  $|S_{train}|/|S| = 0.3$  (C),  $|S_{train}|/|S| = 0.4$  (D),  $|S_{train}|/|S| = 0.5$  (E),  $|S_{train}|/|S| = 0.6$  (F),  $|S_{train}|/|S| = 0.7$  (G),  $|S_{train}|/|S| = 0.8$  (H),  $|S_{train}|/|S| = 0.9$  (I). Gray line represents the expected error of optimal classifier based on Eq. 54.

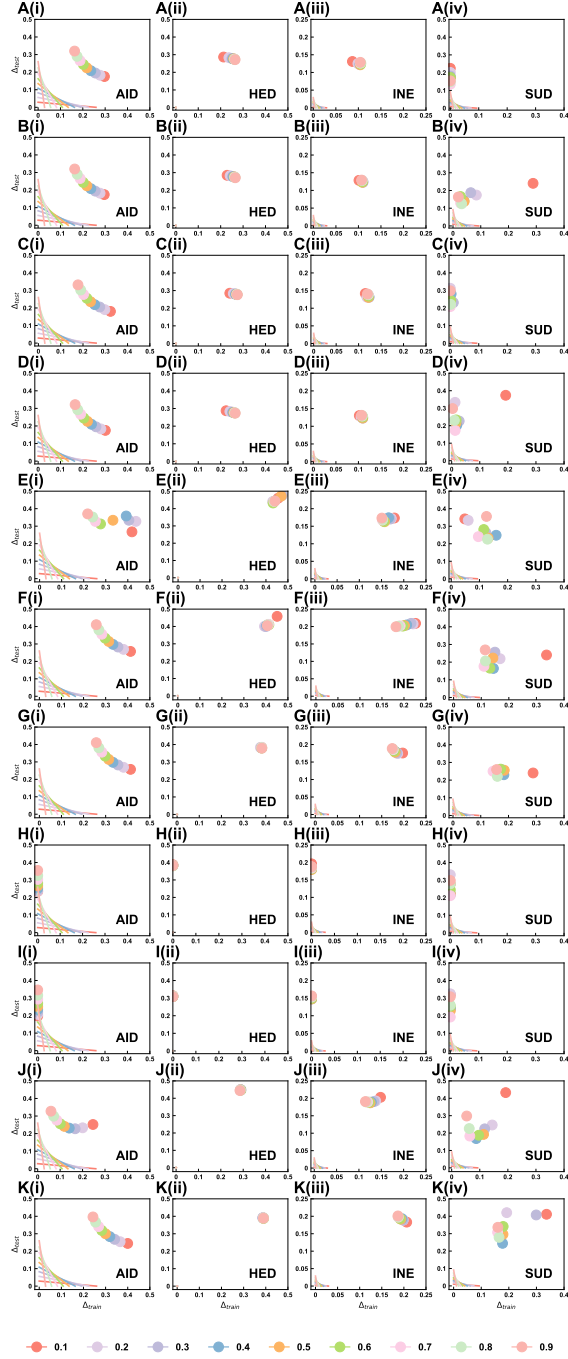


**Fig. S5:** The loss errors of for four datasets (AID, HED, INE and SUD) in training ( $\Delta_{train}^f$ ) and test sets ( $\Delta_{test}^f$ ) of different binary classifiers, including XGBoost with four classical objectives (A-D), MLP (E), SVM (F), Logistic Regression (G), Decision Tree (H), Random Forest (I), KNN (J). Colorful dots and lines represent different  $|\mathcal{S}_{train}|/|\mathcal{S}|$  ranging from 0.1 to 0.9.

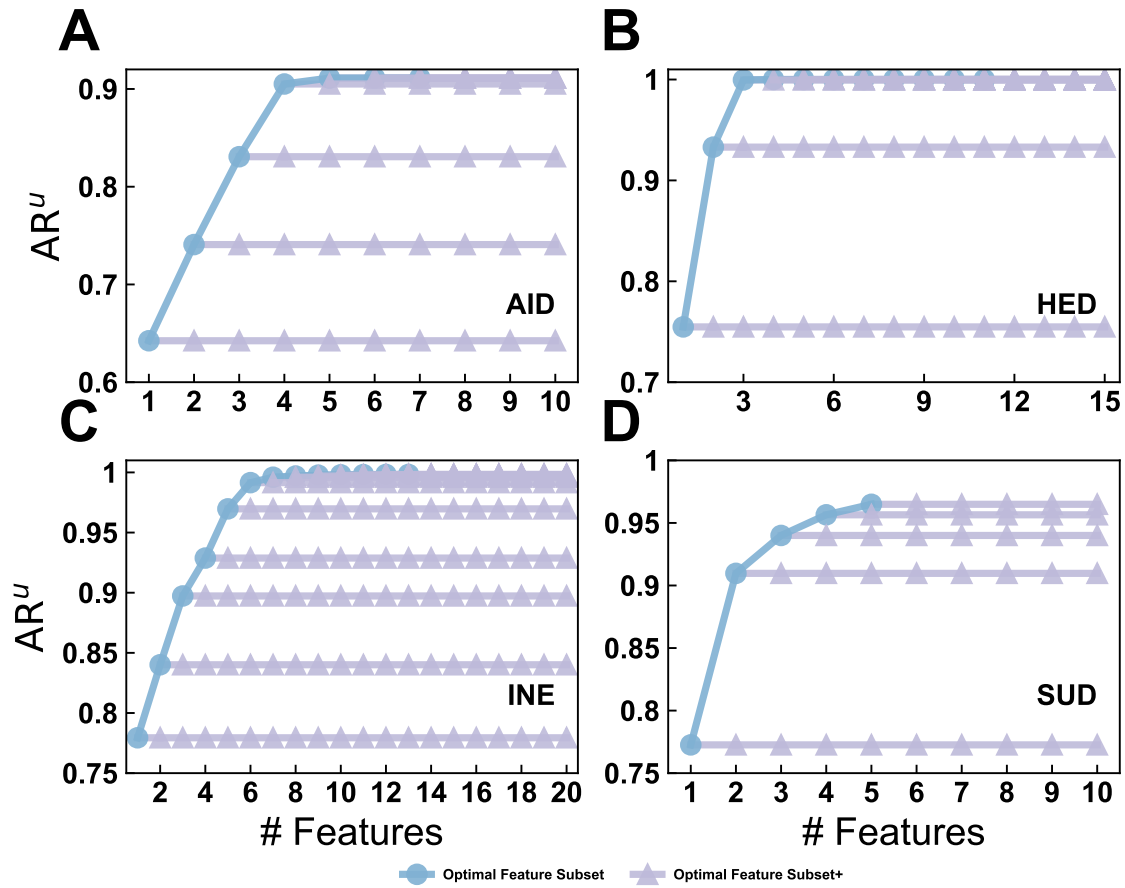


**Fig. S6:** The  $AR^u_{k_0}$  versus the optimal  $k_0$  feature subset in feature selection (blue lines and dots). After we selected the optimal  $k_0$  feature subset, we would use the feature extraction skill (LDA) to create new extracted features and add them into the original  $k_0$  feature one by one (see red lines and dots). The datasets we used in this experiment includes AID (A), HED (B), INE (C) and SUD (D).

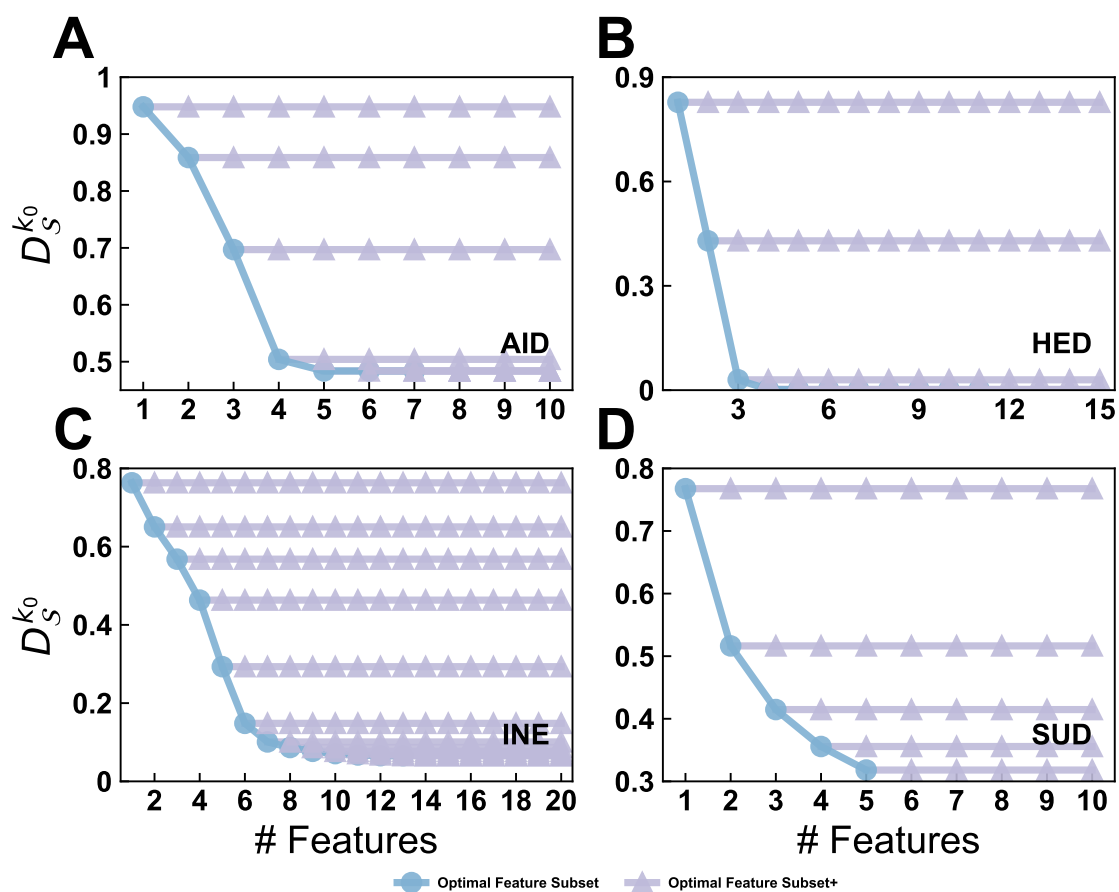


**Fig. S7:** The  $D_S^{k_0}$  versus the optimal  $k_0$  feature subset in feature selection (blue lines and dots). After we selected the optimal  $k_0$  feature subset, we would use the feature extraction skill (LDA) to create new extracted features and add them into the original  $k_0$  feature one by one (see red lines and dots). The datasets we used in this experiment includes AID (A), HED (B), INE (C) and SUD (D).

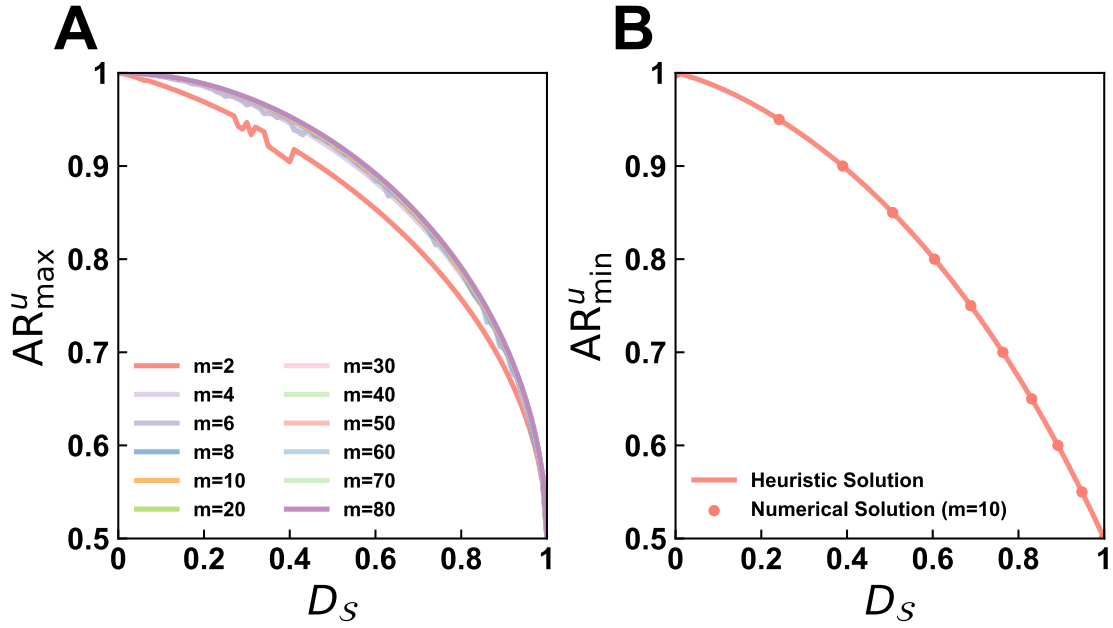


**Fig. S8:**  $AR^u_{\max}(D_S)$  curve (A) and  $AR^u_{\min}(D_S)$  curve (B). (A)  $AR^u_{\max}(D_S)$  curves is numerically solved by the SLSQP solver when  $m = 2, 4, 6, 8, 10, 20, 30, 40, 50, 60, 70, 80$ . We find that these curves are quickly converged as  $m$  increases. Therefore the final  $AR^u_{\max}(D_S)$  curve can be approximated to the numerically solved curve when  $m = 10$ . (B) The heuristic curve for  $AR^u_{\min}(D_S)$  is calculated by (68). And the numerically approximated  $AR^u_{\min}(D_S)$  curve is derived by the SLSQP solver. These two solution happens to match each other. So we utilize (68) to approximate  $AR^u_{\min}$  curve.